Structure of the deuteron from an analysis of bremsstrahlung emission in proton-deuteron scattering in cluster models

K. A. Shaulskyi,[1,*] S. P. Maydanyuk,[1,2,†] and V. S. Vasilevsky[3,‡]
[1]*Institute for Nuclear Research, National Academy of Sciences of Ukraine, Kyiv 03680, Ukraine*
[2]*Wigner Research Centre for Physics, Budapest 1121, Hungary*
[3]*Bogolyubov Institute for Theoretical Physics, Metrolohichna Street 14b, Kyiv 03143, Ukraine*

(Received 30 April 2024; accepted 24 July 2024; published 4 September 2024)

Background: Emission of bremsstrahlung photons in the scattering of protons off deuterons is investigated on the microscopic cluster basis in a wide region of beam energy from low energies up to 1.5 GeV.
Purpose: Our aim is to construct a model extracting new information about the structure of the deuteron from analysis of accompanying bremsstrahlung in proton-deuteron scattering.
Methods: A three-cluster model of bremsstrahlung is constructed. The formalism includes the form factor of the deuteron, which characterizes the dependence of bremsstrahlung cross sections on the structure of the deuteron. This gives a possibility to investigate the structure of nuclei from analysis of bremsstrahlung cross sections.
Results: We studied the dependence of the bremsstrahlung cross section on the structure of the deuteron. We used three different shapes of the deuteron wave functions. Besides, we also calculated the cross section by neglecting the internal structure of the deuteron. Analysis of the dependence of the cross section on such a parameter shows the following. (1) At beam energies 145 and 195 MeV used in experiments, the bremsstrahlung cross section is not sensitive enough to variations in the shape of the deuteron wave functions. (2) A stable difference between cross sections calculated with and without the internal structure of the deuteron is observed at higher bean energy (higher than 500 MeV). (3) The spectrum is increased as we pass from the structureless deuteron (the oscillator length $b = 0$) to the deuteron described by the shell-model wave function (the realistic oscillator length) inside the full energy region of the emitted photons.
Conclusions: Our cluster model is a suitable tool to study the structure of the deuteron with high enough precision from bremsstrahlung analysis. We propose new experiments for such an investigation.

DOI: 10.1103/PhysRevC.110.034001

I. INTRODUCTION

The bremsstrahlung emission of photons accompanying nuclear reactions is an important topic of nuclear physics and has attracted the significant interest of many researchers for a long time (see reviews [1–4]). This is explained by the spectra of bremsstrahlung photons being calculated based on nuclear models which include mechanisms of reactions, interactions between nuclei, dynamics, and many other physical issues. A lot of aspects of nuclear processes, such as dynamics of nucleons in nuclear scattering, interactions between nucleons, mechanisms of reactions, quantum effects, deformations of nuclei, properties of hypernuclei in reactions, etc. can be included in the model describing the bremsstrahlung emission (for example, see Refs. [5,6] for general properties of α decay from bremsstrahlung analysis, Ref. [7] for extraction of information about deformation of nuclei in α decay from experimental bremsstrahlung data, Ref. [8] for bremsstrahlung in the nuclear radioactivity with emission of protons, Ref. [9] for bremsstrahlung in the spontaneous fission of ^{252}Cf, Ref. [10] for bremsstrahlung in the ternary fission of ^{252}Cf, and Ref. [11] for bremsstrahlung in the pion-nucleus scattering from our research; there are many investigations of other researchers). Note the perspectives on studying electromagnetic observables of light nuclei based on chiral effective field theory [12]. The measurements of photons with analysis provide important information on these phenomena.

Analysis of bremsstrahlung photons accompanying nuclear reactions gives the possibility to extract additional information on the structure of nuclei. The study of the structure of nuclei based on bremsstrahlung analysis is one of the most ambitious aims in nuclear physics. Analyzing the formalism of models, the option to investigate the structure of nuclei exists, in principle, and is understandable. The study of the structure of nuclei is one of the most promising research directions, taking into account that photons can be measured in experiments. However, during the long period of

*Contact author: shaulskyi@kinr.kiev.ua
†Contact author: sergei.maydanyuk@wigner.hu
‡Contact author: vsvasilevsky@gmail.com

investigations of bremsstrahlung photons in nuclear physics, a systematic study of the structure of nuclei has not been realized yet. One can explain this by the difficulty in the development of a mathematical formalism of models, and it is important to reach the stability of numerical calculations that is possible at high precision. Moreover, it turns out that not all available experimental bremsstrahlung data are very sensitive to the structure of nuclei. In this regards, one can recall investigations of bremsstrahlung emission in reactions with light nuclei within microscopic two-cluster models [13–27].

Summarizing all issues above, we conclude that realization of such an idea is a perspective task. So, this is the main idea of the paper. We would like to understand which parameters of nuclear structure are more effective to realize such an investigation. Of course, the best way is to construct this model on a fully quantum basis, with the inclusion of realistic nuclear interactions which were well tested experimentally. A promising way is the cluster formalism for the description of structure of nuclei and nuclear process. So, as a basis of this research we will develop fully the cluster model in combination with a bremsstrahlung formalism. The most effective process for such a study is proton-deuteron scattering, so we will focus on the reaction $p+d \to p'+d'+\gamma$ in this paper. We focus on the construction of such a unified cluster formalism, and analysis of available experimental information about bremsstrahlung for proton-deuteron scattering. This paper is a continuation of our previous research [28], where we developed a cluster model in the folding approximation in the study of bremsstrahlung emission in the scattering of nuclei with a small number of nucleons and we did not analyze the possibility of extracting information about the structure of nuclei from bremsstrahlung cross sections.

The paper is organized in the following way. In Sec. II cluster models of emission of the bremsstrahlung photons in the proton-deuteron scattering are formulated. Here, we give an explicit form of the operator of the bremsstrahlung emission, define wave functions of the $p+d$ system, calculate matrix elements of bremsstrahlung emission, define form factors of the deuteron (characterizing its structure), and apply the multiple expansion approach for the calculation of matrix elements. In Sec. II K matrix elements of bremsstrahlung emission in the folding approximation are reviewed (following the formalism in Ref. [28]). In Sec. II L the cross section of the bremsstrahlung emission of photons is determined and resulting formulas are summarized. In Sec. III emission of the bremsstrahlung photons for the proton-deuteron scattering is studied based on the model above. We analyze the role of the deuteron wave function and its form factor in calculations of the cross section at different energies of relative motions between the scattered proton and deuteron. We also describe the experimental bremsstrahlung data for proton-deuteron scattering based on the model. Conclusions and perspectives are summarized in Sec. IV. The operator of the bremsstrahlung emission in the three-cluster model is calculated in Appendix A. Useful details of the calculation of integrals are presented in Appendix B.

II. BREMSSTRAHLUNG EMISSION IN TWO- AND THREE-CLUSTER MODELS

A. Operator of the bremsstrahlung emission in a three-cluster model

Consider the translationally invariant interaction of a photon with a three-nucleon system,

$$\widehat{H}_e(\mathbf{k}_\gamma, \varepsilon^{(\alpha)}) = \frac{1}{2}\frac{e\hbar}{m_N c}\sum_{i=1}^{A=3}\frac{1}{2}(1+\widehat{\tau}_{iz})[\widehat{\pi}_i^* \mathbf{A}^*(i) + \mathbf{A}^*(i)\widehat{\pi}_i^*], \tag{1}$$

where

$$\mathbf{A}^*(i) = \varepsilon^{(\alpha)}\exp\{-i(\mathbf{k}_\gamma \rho_i)\}, \quad \widehat{\pi}_i^* = i\nabla_{\rho_i},$$
$$\rho_i = \mathbf{r}_i - \mathbf{R}_{\rm cm}, \quad \mathbf{R}_{\rm cm} = \frac{1}{A}\sum_{i=1}^{A}\mathbf{r}_i,$$
$$\widehat{\pi}_i = \widehat{\mathbf{p}}_i - \widehat{\mathbf{P}}_{\rm cm}, \quad \widehat{\mathbf{P}}_{\rm cm} = \frac{1}{A}\sum_{i=1}^{A}\widehat{\mathbf{p}}_i. \tag{2}$$

Here and below, an asterisk symbol $*$ means complex conjugation. In Eq. (1), $\boldsymbol{\varepsilon}^{(\alpha)}$ are unit vectors of *linear* polarization of the photon emitted ($\boldsymbol{\varepsilon}^{(\alpha),*} = \boldsymbol{\varepsilon}^{(\alpha)}$), $\mathbf{k}_\gamma$ is the wave vector of the photon, and $w_\gamma = k_\gamma c = |\mathbf{k}_\gamma| c$. Vectors $\boldsymbol{\varepsilon}^{(\alpha)}$ are perpendicular to $\mathbf{k}_\gamma$ in the Coulomb gauge. We have two independent polarizations $\boldsymbol{\varepsilon}^{(1)}$ and $\boldsymbol{\varepsilon}^{(2)}$ for the photon with impulse $\mathbf{k}_\gamma$ ($\alpha = 1, 2$). Also we have properties

$$[\mathbf{k}_\gamma \times \boldsymbol{\varepsilon}^{(1)}] = k_\gamma\, \boldsymbol{\varepsilon}^{(2)}, \quad [\mathbf{k}_\gamma \times \boldsymbol{\varepsilon}^{(2)}] = -k_\gamma\, \boldsymbol{\varepsilon}^{(1)},$$
$$[\mathbf{k}_\gamma \times \boldsymbol{\varepsilon}^{(3)}] = 0, \quad \sum_{\alpha=1,2,3}[\mathbf{k}_\gamma \times \boldsymbol{\varepsilon}^{(\alpha)}] = k_\gamma\,(\boldsymbol{\varepsilon}^{(2)} - \boldsymbol{\varepsilon}^{(1)}). \tag{3}$$

Let us introduce new variables, namely Jacobi vectors $\mathbf{r}$ and $\mathbf{q}$:

$$\mathbf{r} = \frac{1}{\sqrt{2}}(\rho_1 - \rho_2) = \frac{1}{\sqrt{2}}(\mathbf{r}_1 - \mathbf{r}_2),$$
$$\mathbf{q} = \sqrt{\frac{2}{3}}\left(\rho_3 - \frac{\rho_1+\rho_2}{2}\right) = \sqrt{\frac{2}{3}}\left(\mathbf{r}_3 - \frac{\mathbf{r}_1+\mathbf{r}_2}{2}\right),$$
$$\mathbf{q}_A = \sqrt{\frac{1}{3}}(\mathbf{r}_1+\mathbf{r}_2+\mathbf{r}_3) = \sqrt{3}\mathbf{R}_{\rm cm}.$$

Inverse relations are

$$\mathbf{r}_1 = \frac{1}{\sqrt{2}}\mathbf{r} - \frac{1}{\sqrt{6}}\mathbf{q} + \frac{1}{\sqrt{3}}\mathbf{q}_A,$$
$$\mathbf{r}_2 = -\frac{1}{\sqrt{2}}\mathbf{r} - \frac{1}{\sqrt{6}}\mathbf{q} + \frac{1}{\sqrt{3}}\mathbf{q}_A,$$
$$\mathbf{r}_3 = \sqrt{\frac{2}{3}}\mathbf{q} + \frac{1}{\sqrt{3}}\mathbf{q}_A. \tag{4}$$

Similar relations can be written for momenta

$$\pi_{\mathbf{r}} = \frac{1}{\sqrt{2}}(\pi_1 - \pi_2), \quad \pi_{\mathbf{q}} = \sqrt{\frac{2}{3}}\left(\pi_3 - \frac{\pi_1+\pi_2}{2}\right),$$
$$\pi_A = \sqrt{\frac{1}{3}}(\pi_1+\pi_2+\pi_3).$$

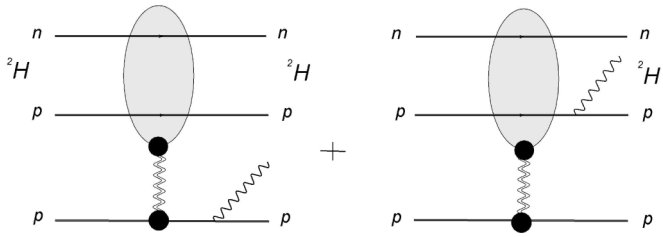

FIG. 1. Diagrammatic representation of the emission of the bremsstrahlung photons during the scattering of the proton on deuteron.

Inverse relations

$$\pi_1 = \frac{1}{\sqrt{2}}\pi_{\mathbf{r}} - \frac{1}{\sqrt{6}}\pi_{\mathbf{q}} + \frac{1}{\sqrt{3}}\pi_A,$$
$$\pi_2 = -\frac{1}{\sqrt{2}}\pi_{\mathbf{r}} - \frac{1}{\sqrt{6}}\pi_{\mathbf{q}} + \frac{1}{\sqrt{3}}\pi_A,$$
$$\pi_3 = \sqrt{\frac{2}{3}}\pi_{\mathbf{q}} + \frac{1}{\sqrt{3}}\pi_A.$$

Now we fix the position of nucleons. We assume that vector $\mathbf{r}$ measures the distance between proton and neutron which form a deuteron. We also assume that $\mathbf{r}_1$ is a coordinate of the first proton and $\mathbf{r}_2$ is a coordinate of a neutron. Vector $\mathbf{r}_3$ determines the location of the second proton. With such definitions, the operator $\widehat{H}_e(\mathbf{k}_\gamma, \varepsilon^{(\alpha)})$ is [see Appendix A for details; also we take into account that $(\varepsilon^{(\alpha)}, \mathbf{k}_\gamma) = 0$]

$$\widehat{H}_e(\mathbf{k}_\gamma, \varepsilon^{(\alpha)}) = \frac{1}{2}\frac{e\hbar}{m_N c}\left\{\frac{2}{\sqrt{2}}\exp\left\{-i\frac{1}{\sqrt{2}}(\mathbf{k}_\gamma\mathbf{r})\right\}(\varepsilon^{(\alpha)}, \pi^*_{\mathbf{r}})\right.$$
$$\times \exp\left\{i\frac{1}{\sqrt{6}}(\mathbf{k}_\gamma\mathbf{q})\right\} - \sqrt{\frac{2}{3}}\exp\left\{-i\frac{1}{\sqrt{2}}(\mathbf{k}_\gamma\mathbf{r})\right\}$$
$$\times \exp\left\{i\frac{1}{\sqrt{6}}(\mathbf{k}_\gamma\mathbf{q})\right\}(\varepsilon^{(\alpha)}, \pi^*_{\mathbf{q}}) + 2\sqrt{\frac{2}{3}}$$
$$\left.\times \exp\left\{-i\sqrt{\frac{2}{3}}(\mathbf{k}_\gamma\mathbf{q})\right\}(\varepsilon^{(\alpha)}, \pi^*_{\mathbf{q}})\right\}. \quad (5)$$

This is the universal and model-independent form of the operator of the bremsstrahlung emission for a system comprising two protons and one neutron. The diagrammatic representation of the emission of the bremsstrahlung photons in the proton-deuteron scattering is depicted in Fig. 1.

To calculated cross section of bremsstrahlung emission in the process of a proton scattering from a deuteron, we need to formulate model which provides a realistic description of the $p + d$ scattering in an economical way, i.e., with the minimum of computations but with a reliable output. As the output, we need to determine wave functions of the $p + d$ scattering at selected energies of initial and final states of bremsstrahlung emission. For this aim, we select the resonating group method (RGM), which is the most rigorous and self-consistent realization of a cluster model. We will use three different variants of the RGM: two- and three-cluster variants and the so-called folding approximation. These three variants of the RGM are explained in detail in the next section.

B. Two- and three-cluster models of the $p + d$ system

The three-nucleon system ^{3}He and its decay channel $p + d$ will be studied in the framework of two- and three-cluster models. In a two-cluster model, the wave function of the system is

$$\Psi = \widehat{\mathcal{A}}\{\phi^{(S)}(d, \mathbf{r})\phi(p)\psi_E(\mathbf{q})\}, \quad (6)$$

where $\phi^{(S)}(d, \mathbf{r})$ is the deuteron wave function from the oscillator shell model, $\phi(p)$ is a wave function of the proton represented by its spin and isospin parts, and $\psi_E(\mathbf{q})$ is a wave function of the relative motion of the proton and deuteron. The antisymmetrization operator $\widehat{\mathcal{A}}$ makes wave functions of the $p + d$ system fully antisymmetric. The three-cluster model suggests the following form for a three-nucleon system:

$$\Psi = \widehat{\mathcal{A}}\{\phi(n)\phi(p_1)\phi(p_2)f(\mathbf{r}, \mathbf{q})\}, \quad (7)$$

The wave function $\phi(p_2)f(\mathbf{r}, \mathbf{q})$ of the relative motion of nucleons has to be determined by solving the Schrödinger equation or the Faddeev equations.

By assuming that the shape of a deuteron does not change when a proton is approaching, the three-particle wave function can be represented as

$$\Psi = \widehat{\mathcal{A}}\{\phi(d, \mathbf{r})\phi(p)\psi_E(\mathbf{q})\}, \quad (8)$$

where $\phi(d, \mathbf{r})$ is a wave function of the bound state of deuteron. The wave function $\phi(d, \mathbf{r})$ is a solution of the two-body Schrödinger equation with selected nucleon-nucleon potential.

Note that in both two-cluster and three-cluster models the wave function of the deuteron is assumed to be antisymmetric, so the antisymmetrization operator $\widehat{\mathcal{A}}$ in Eqs. (6) and (8) consists of the unit operator and two permutation operators. As a result, the antisymmetrization operator $\widehat{\mathcal{A}}$ creates three terms in Eqs. (6) and (8) that are similar to the terms in curly brackets.

If one ignores the full antisymmetrization in Eqs. (6) and (8) by omitting the operator $\widehat{\mathcal{A}}$, one obtains a simple version of the two- and three-cluster models which is called a folding approximation or folding model. To avoid bulky expressions, we will use this approximation to present matrix elements of $\widehat{H}_e(\mathbf{k}_\gamma, \varepsilon_\mu)$ between the initial and final states of the $p + d$ system.

To construct wave functions of the system $p + d$ in different approximations (models), we need to solve the appropriate Schrödinger equations. For this aim we employ the algebraic version of the resonating group method (RGM), formulated in Refs. [29,30]. This version of the RGM uses the full basis of oscillator functions to expand wave functions of the relative motion of clusters. As a result, the Schrödinger equation is reduced to a system of linear algebraic equations for expansion coefficients. Besides, the algebraic version implements proper boundary conditions in discrete, oscillator representation.

To study the $p + d$ system in a three-cluster approximation, we will employ a three-cluster model developed in Ref. [31].

C. Wave functions of the $p + d$ system in the cluster formalism

We need to construct wave functions of the $p + d$ system to calculate matrix elements of the operator $\widehat{H}_e(\mathbf{k}_\gamma, \varepsilon^{(\alpha)})$. If

we neglect the Pauli principle and employ an adiabatic approximation, then the wave function of the system can be constructed in a separable form,

$$\Psi(\mathbf{r},\mathbf{q}) = \phi(\mathbf{r})\psi(\mathbf{q}), \tag{9}$$

where wave function of the deuteron, $\phi(\mathbf{r})$, is a solution of the two-body Schrödinger equation

$$(\widehat{H}_d - E_d)\phi(\mathbf{r}) = 0, \tag{10}$$

$$\widehat{H}_d = -\frac{\hbar^2}{2m}\frac{d^2}{d\mathbf{r}^2} + \widehat{V}_{NN}(\mathbf{r}) \tag{11}$$

where m is the mass of nucleon. If the nucleon-nucleon potential $V_{NN}(\mathbf{r})$ is used in the form

$$\widehat{V}_{NN}(\mathbf{r}) = \sum_{S=0,1}\sum_{T=0,1} V_{2S+1,2T+1}(\mathbf{r})\widehat{P}_S\widehat{P}_T, \tag{12}$$

where $\widehat{P}_S$ ($\widehat{P}_T$) is the projection operator projecting onto the spin S (the isospin T) of the two-nucleon system, then in Eq. (11) $\widehat{V}_{NN}(\mathbf{r})$ should be replaced with the even component $V_{31}(\mathbf{r})$, as the deuteron has spin $S = 1$ and isospin $T = 0$.

The wave function which describes the interaction of the proton with the deuteron obeys the equation

$$(\widehat{H}_p - E_p)\psi(\mathbf{q}) = 0, \tag{13}$$

where

$$\widehat{H}_p = -\frac{\hbar^2}{2m}\frac{d^2}{d\mathbf{q}^2} + \widehat{V}_{pd}(\mathbf{q})$$

and the potential energy $\widehat{V}_{pd}(\mathbf{q})$ equals

$$\widehat{V}_{pd}(\mathbf{q}) = \langle\phi(\mathbf{r})|\sum_{i=1,2}\widehat{V}_{NN}(\mathbf{r}_3 - \mathbf{r}_i) + \sum_{i=1,2}\widehat{V}_C(\mathbf{r}_3 - \mathbf{r}_i)|\phi(\mathbf{r})\rangle.$$

Here, integration is performed over vector $\mathbf{r}$, and nucleon-nucleon $\widehat{V}_{NN}$ and Coulomb $\widehat{V}_C$ potentials are involved in the definition of $\widehat{V}_{pd}(\mathbf{q})$. Equation (13) determines both the initial $\psi_{E_i}(\mathbf{q})$ and final $\psi_{E_f}(\mathbf{q})$ wave functions of the $p+d$ system.

D. Matrix elements of bremsstrahlung emission in the cluster formalism

Based on assumptions made, we have the matrix element of transitions from initial to final states

$$\langle\phi(\mathbf{r})\psi_{E_f}(\mathbf{q})|\widehat{H}_e(\mathbf{k}_\gamma,\varepsilon^{(\alpha)})|\phi(\mathbf{r})\psi_{E_i}(\mathbf{q})\rangle.$$

We suggest calculating these matrix elements in two steps. In the first step, we calculate the matrix element

$$\widehat{\mathcal{H}}_e(\mathbf{q}) = \langle\phi(\mathbf{r})|\widehat{H}_e(\mathbf{k}_\gamma,\varepsilon^{(\alpha)})|\phi(\mathbf{r})\rangle$$

by integrating over vector $\mathbf{r}$. By using Eq. (5), we obtain

$$\begin{aligned}\widehat{\mathcal{H}}_e(\mathbf{q}) &= \langle\phi(\mathbf{r})|\widehat{H}_e(\mathbf{k}_\gamma,\varepsilon^{(\alpha)})|\phi(\mathbf{r})\rangle\\ &= \frac{1}{2}\frac{e\hbar}{m_N c}\left\{\frac{2}{\sqrt{2}}\langle\phi(\mathbf{r})|\exp\left\{-i\frac{1}{\sqrt{2}}(\mathbf{k}_\gamma\mathbf{r})\right\}(\varepsilon^{(\alpha)},\pi^*_{\mathbf{r}})\right.\\ &\quad\times|\phi(\mathbf{r})\rangle\exp\left\{i\frac{1}{\sqrt{6}}(\mathbf{k}_\gamma\mathbf{q})\right\}\\ &\quad-\sqrt{\frac{2}{3}}\langle\phi(\mathbf{r})|\exp\left\{-i\frac{1}{\sqrt{2}}(\mathbf{k}_\gamma\mathbf{r})\right\}|\phi(\mathbf{r})\rangle\\ &\quad\times\exp\left\{i\frac{1}{\sqrt{6}}(\mathbf{k}_\gamma\mathbf{q})\right\}(\varepsilon^{(\alpha)},\pi^*_{\mathbf{q}})\\ &\quad\left.+\,2\sqrt{\frac{2}{3}}\exp\left\{-i\sqrt{\frac{2}{3}}(\mathbf{k}_\gamma\mathbf{q})\right\}(\varepsilon^{(\alpha)},\pi^*_{\mathbf{q}})\right\}\end{aligned} \tag{14}$$

and then

$$\begin{aligned}&\langle\phi(\mathbf{r})\psi_{E_f}(\mathbf{q})|\widehat{H}_e(\mathbf{k}_\gamma,\varepsilon^{(\alpha)})|\phi(\mathbf{r})\psi_{E_i}(\mathbf{q})\rangle\\ &\quad= \frac{1}{2}\frac{e\hbar}{m_N c}\left\{\frac{2}{\sqrt{2}}\langle\phi(\mathbf{r})|\exp\left\{-\frac{i}{\sqrt{2}}(\mathbf{k}_\gamma\mathbf{r})\right\}(\varepsilon^{(\alpha)},\pi^*_{\mathbf{r}})|\phi(\mathbf{r})\rangle\right.\\ &\qquad\times\langle\psi_{E_f}(\mathbf{q})|\exp\left\{\frac{i}{\sqrt{6}}(\mathbf{k}_\gamma\mathbf{q})\right\}|\psi_{E_i}(\mathbf{q})\rangle\\ &\qquad-\sqrt{\frac{2}{3}}\langle\phi(\mathbf{r})|\exp\left\{-\frac{i}{\sqrt{2}}(\mathbf{k}_\gamma\mathbf{r})\right\}|\phi(\mathbf{r})\rangle\langle\psi_{E_f}(\mathbf{q})|\\ &\qquad\times\exp\left\{\frac{i}{\sqrt{6}}(\mathbf{k}_\gamma\mathbf{q})\right\}(\varepsilon^{(\alpha)},\pi^*_{\mathbf{q}})|\psi_{E_i}(\mathbf{q})\rangle + 2\sqrt{\frac{2}{3}}\langle\psi_{E_f}(\mathbf{q})|\\ &\qquad\left.\times\exp\left\{-i\sqrt{\frac{2}{3}}(\mathbf{k}_\gamma\mathbf{q})\right\}(\varepsilon^{(\alpha)},\pi^*_{\mathbf{q}})|\psi_{E_i}(\mathbf{q})\rangle\right\}.\end{aligned} \tag{15}$$

Thus we need to calculate a few basic integrals:

$$\begin{aligned}&\langle\phi(\mathbf{r})|\exp\left\{-\frac{i}{\sqrt{2}}(\mathbf{k}_\gamma\mathbf{r})\right\}|\phi(\mathbf{r})\rangle,\\ &\langle\phi(\mathbf{r})|\exp\left\{-\frac{i}{\sqrt{2}}(\mathbf{k}_\gamma\mathbf{r})\right\}(\varepsilon^{(\alpha)},\pi^*_{\mathbf{r}})|\phi(\mathbf{r})\rangle,\\ &\langle\psi_{E_f}(\mathbf{q})|\exp\left\{\frac{i}{\sqrt{6}}(\mathbf{k}_\gamma\mathbf{q})\right\}|\psi_{E_i}(\mathbf{q})\rangle,\\ &\langle\psi_{E_f}(\mathbf{q})|\exp\left\{\frac{i}{\sqrt{6}}(\mathbf{k}_\gamma\mathbf{q})\right\}(\varepsilon^{(\alpha)},\pi^*_{\mathbf{q}})|\psi_{E_i}(\mathbf{q})\rangle.\end{aligned} \tag{16}$$

Note that with such a definition of coordinates (4), the wave vectors of initial and final states are defined as $k_i = \sqrt{2mE_i/\hbar^2}$, $k_f = \sqrt{2mE_f/\hbar^2}$, where energies E_i and E_f are in MeV and are in the center-of-mass motion.

E. Introduction of form factors

We introduce the following definitions of *form factors of the deuteron* (in the formalism of the three-cluster model):

$$\begin{aligned}F_1(\mathbf{k}_\gamma) &= \langle\phi(\mathbf{r})|\exp\left\{-\frac{i}{\sqrt{2}}(\mathbf{k}_\gamma\mathbf{r})\right\}|\phi(\mathbf{r})\rangle,\\ F_{2,\alpha}(\mathbf{k}_\gamma) &= \langle\phi(\mathbf{r})|\exp\left\{-\frac{i}{\sqrt{2}}(\mathbf{k}_\gamma\mathbf{r})\right\}(\varepsilon^{(\alpha)},\pi^*_{\mathbf{r}})|\phi(\mathbf{r})\rangle.\end{aligned} \tag{17}$$

Then, the matrix element of emission in Eq. (15) is rewritten as

$$\begin{aligned}&\langle\Psi_{E_f}(\mathbf{r},\mathbf{q})|\hat{H}_\gamma(\mathbf{k}_\gamma,\varepsilon^{(\alpha)})|\Psi_{E_i}(\mathbf{r},\mathbf{q})\rangle\\ &\quad= \frac{1}{2}\frac{e\hbar}{m_N c}\left(\frac{2}{\sqrt{2}}\langle\psi_{E_f}(\mathbf{q})|\exp\left\{\frac{i}{\sqrt{6}}(\mathbf{k}_\gamma\mathbf{q})\right\}|\phi_{E_i}(\mathbf{q})\rangle F_{2,\alpha}\right.\end{aligned}$$

$$- \sqrt{\frac{2}{3}} \left\langle \psi_{E_f}(\mathbf{q}) \right| \exp\left\{ \frac{i}{\sqrt{6}} (\mathbf{k}_\gamma \mathbf{q}) \right\} (\varepsilon^{(\alpha)}, \pi^*_{\mathbf{q}}) \left| \psi_{E_i}(\mathbf{q}) \right\rangle$$
$$F_1 \; + 2 \sqrt{\frac{2}{3}} \left\langle \varphi_{E_f}(\mathbf{q}) \right| \exp\left\{ - i \sqrt{\frac{2}{3}} (\mathbf{k}_\gamma \mathbf{q}) \right\}$$
$$\times (\varepsilon^{(\alpha)}, \pi^*_{\mathbf{q}}) \left| \varphi_{E_i}(\mathbf{q}) \right\rangle \Big), \tag{18}$$

where

$$\Psi_{E_i}(\mathbf{r}, \mathbf{q}) = \phi(\mathbf{r}) \psi_{E_i}(\mathbf{q}), \tag{19}$$

$$\Psi_{E_f}(\mathbf{r}, \mathbf{q}) = \phi(\mathbf{r}) \psi_{E_f}(\mathbf{q}). \tag{20}$$

We introduce the following notations for matrix elements:

$$\mathbf{I}_1(\alpha) = \left\langle \varphi_{E_f}(\mathbf{q}) \right| e^{-i\alpha \mathbf{k}_\gamma \mathbf{q}} \frac{\partial}{\partial \mathbf{q}} \left| \varphi_{E_i}(\mathbf{q}) \right\rangle_{\mathbf{q}},$$
$$I_2(\alpha) = \left\langle \varphi_{E_f}(\mathbf{q}) \right| e^{-i\alpha \mathbf{k}_\gamma \mathbf{q}} \left| \varphi_{E_i}(\mathbf{q}) \right\rangle_{\mathbf{q}}. \tag{21}$$

Then, the full matrix element (18) can be rewritten as

$$\left\langle \Psi_{E_f}(\mathbf{r}, \mathbf{q}) \right| \hat{H}_\gamma(\mathbf{k}_\gamma, \varepsilon^{(\alpha)}) \left| \Psi_{E_i}(\mathbf{r}, \mathbf{q}) \right\rangle$$
$$= \frac{1}{2} \frac{e\hbar}{m_N c} \Big(\frac{2}{\sqrt{2}} I_2\Big(\frac{-1}{\sqrt{6}}\Big) F_{2,\alpha} - \sqrt{\frac{2}{3}} \left\langle \psi_{E_f}(\mathbf{q}) \right|$$
$$\times \exp\left\{ \frac{i}{\sqrt{6}} (\mathbf{k}_\gamma \mathbf{q}) \right\} (\varepsilon^{(\alpha)}, \pi^*_{\mathbf{q}}) \left| \psi_{E_i}(\mathbf{q}) \right\rangle F_1$$
$$+ 2 \sqrt{\frac{2}{3}} \left\langle \varphi_{E_f}(\mathbf{q}) \right| \exp\left\{ - i \sqrt{\frac{2}{3}} (\mathbf{k}_\gamma \mathbf{q}) \right\}$$
$$\times (\varepsilon^{(\alpha)}, \pi^*_{\mathbf{q}}) \left| \varphi_{E_i}(\mathbf{q}) \right\rangle \Big). \tag{22}$$

Taking into account

$$\pi_{\mathbf{q}} = -i\hbar \frac{\mathbf{d}}{\mathbf{dq}}, \quad \pi^*_{\mathbf{q}} = i\hbar \frac{\mathbf{d}}{\mathbf{dq}}, \tag{23}$$

we rewrite

$$\left\langle \psi_{E_f}(\mathbf{q}) \right| \exp\{\pm i \alpha' (\mathbf{k}_\gamma \mathbf{q})\} (\varepsilon^{(\alpha)}, \pi^*_{\mathbf{q}}) \left| \psi_{E_i}(\mathbf{q}) \right\rangle$$
$$= i\hbar \, \varepsilon^{(\alpha)} \, \mathbf{I}_1(\mp \alpha'). \tag{24}$$

So, the full matrix element (22) obtains the following form:

$$\left\langle \Psi_{E_f}(\mathbf{r}, \mathbf{q}) \right| \hat{H}_\gamma(\mathbf{k}_\gamma, \varepsilon^{(\alpha)}) \left| \Psi_{E_i}(\mathbf{r}, \mathbf{q}) \right\rangle$$
$$= - \frac{1}{2} \frac{e\hbar}{m_N c} \Big\{ \frac{2}{\sqrt{2}} F_{2,\alpha} \cdot I_2\Big(\frac{-1}{\sqrt{6}}\Big) - i\hbar \sqrt{\frac{2}{3}} F_1 \; \varepsilon^{(\alpha)}$$
$$\times \mathbf{I}_1\Big(- \frac{1}{\sqrt{6}}\Big) + 2\, i\hbar \sqrt{\frac{2}{3}} \, \varepsilon^{(\alpha)} \, \mathbf{I}_1\Big(\sqrt{\frac{2}{3}}\Big) \Big\}. \tag{25}$$

Note that vectors $\varepsilon^{(\alpha)}$ are perpendicular to $\mathbf{k}_\gamma$ in the Coulomb gauge. Taking this property into account, we obtain

$$(\varepsilon^{(\alpha)}, \mathbf{k}_\gamma) = 0. \tag{26}$$

In the case of zero form factor $F_{2,\alpha} = 0$, the matrix element is simplified as

$$\left\langle \Psi_{E_f}(\mathbf{r}, \mathbf{q}) \right| \hat{H}_\gamma(\mathbf{k}_\gamma, \varepsilon^{(\alpha)}) \left| \Psi_{E_i}(\mathbf{r}, \mathbf{q}) \right\rangle$$
$$= - i \, \frac{1}{2} \sqrt{\frac{2}{3}} \frac{e\hbar^2}{m_N c} \Big\{ F_1 \, \varepsilon_\mu \, \mathbf{I}_1\Big(- \frac{1}{\sqrt{6}}\Big) - 2 \, \varepsilon^{(\alpha)} \, \mathbf{I}_1\Big(\sqrt{\frac{2}{3}}\Big) \Big\}. \tag{27}$$

F. Multipole expansion

In further calculation of Eq. (27) one needs to find integrals (21). Applying the multipolar expansion, these integrals obtain the form [see Appendix B, Eqs. (B3) and (B6)]

$$\mathbf{I}_1(\alpha) = \left\langle \varphi_{E_f}(\mathbf{q}) \right| e^{-i\alpha \mathbf{k}_\gamma \mathbf{q}} \frac{\partial}{\partial \mathbf{q}} \left| \varphi_{E_i}(\mathbf{q}) \right\rangle_{\mathbf{q}}$$
$$= \sqrt{\frac{\pi}{2}} \sum_{l_\gamma = 1} (-i)^{l_\gamma} \sqrt{2l_\gamma + 1} \sum_{\mu = \pm 1} \xi_\mu \, \mu$$
$$\times \left[p^M_{l_\gamma \mu}(\alpha) - i\mu \, p^E_{l_\gamma \mu}(\alpha) \right],$$
$$I_2(\alpha) = \left\langle \varphi_{E_f}(\mathbf{q}) \right| e^{-i\alpha \mathbf{k}_\gamma \mathbf{q}} \left| \varphi_{E_i}(\mathbf{q}) \right\rangle_{\mathbf{q}}$$
$$= \sqrt{\frac{\pi}{2}} \sum_{l_\gamma = 1} (-i)^{l_\gamma} \sqrt{2l_\gamma + 1} \sum_{\mu = \pm 1}$$
$$\times \left[\mu \, \tilde{p}^M_{l_\gamma \mu}(\alpha) - i \, \tilde{p}^E_{l_\gamma \mu}(\alpha) \right], \tag{28}$$

where [see Eqs. (B4) and (B7)]

$$p^M_{l_\gamma \mu}(\alpha) = -I_M(0, l_f, l_\gamma, 1, \mu) J_1(\alpha, 0, l_f, l_\gamma),$$
$$p^E_{l_\gamma \mu}(\alpha) = \sqrt{\frac{l_C + 1}{2l_\gamma + 1}} I_E(0, l_f, l_\gamma, 1, l_\gamma - 1, \mu)$$
$$J_1(\alpha, 0, l_f, l_\gamma - 1)$$
$$- \sqrt{\frac{l_\gamma}{2l_\gamma + 1}} I_E(0, l_f, l_\gamma, 1, l_\gamma + 1, \mu)$$
$$J_1(\alpha, 0, l_f, l_\gamma + 1), \tag{29}$$
$$\tilde{p}^M_{l_\gamma \mu}(\alpha) = \tilde{I}(0, l_f, l_\gamma, l_\gamma, \mu) \tilde{J}(\alpha, 0, l_f, l_\gamma),$$
$$\tilde{p}^E_{l_\gamma \mu}(\alpha) = \sqrt{\frac{l_\gamma + 1}{2l_\gamma + 1}} \tilde{I}(0, l_f, l_\gamma, l_\gamma - 1, \mu) \tilde{J}(\alpha, 0, l_f, l_\gamma - 1)$$
$$- \sqrt{\frac{l_\gamma}{2l_\gamma + 1}} \tilde{I}(0, l_f, l_\gamma, l_\gamma + 1, \mu)$$
$$\tilde{J}(\alpha, 0, l_f, l_\gamma + 1), \tag{30}$$

and [see Eqs. (B5) and (B8)]

$$J_1(\alpha, l_i, l_f, n) = \int_0^{+\infty} \frac{dR_i(r, l_i)}{dr} R^*_f(l_f, r) \, j_n(\alpha \, kr) \, r^2 dr,$$
$$\tilde{J}(\alpha, l_i, l_f, n) = \int_0^{+\infty} R_i(r) R^*_f(l, r) \, j_n(\alpha k_\gamma r) \, r^2 dr. \tag{31}$$

Here, ξ_μ are *vectors of circular polarization* with opposite directions of rotation (see Ref. [32], Eq. (2.39), p. 42). Also

we have the following properties [see Appendix B, Eqs. (B20) and (B21)]

$$\sum_{\alpha=1,2} \boldsymbol{\varepsilon}^{(\alpha)} \cdot \mathbf{I}_1 = \sqrt{\frac{\pi}{2}} \sum_{l_\gamma=1} (-i)^{l_\gamma} \sqrt{2l_\gamma+1} \times \sum_{\mu=\pm1} \mu\, h_\mu \left(p^M_{l_\gamma,\mu} + p^E_{l_\gamma,-\mu}\right),$$
$$(\boldsymbol{\varepsilon}_x + \boldsymbol{\varepsilon}_z) \sum_{\alpha=1,2} [\mathbf{I}_1 \times \boldsymbol{\varepsilon}^{(\alpha)}] = \sqrt{\frac{\pi}{2}} \sum_{l_\gamma=1} (-i)^{l_\gamma} \sqrt{2l_\gamma+1} \times \sum_{\mu=\pm1} \mu\, h_\mu \left(p^M_{l_\gamma,\mu} - p^E_{l_\gamma,-\mu}\right), \tag{32}$$

where [see Appendix B, Eqs. (B10)]

$$h_\pm = \mp\frac{1 \pm i}{\sqrt{2}}, \quad h_- + h_+ = -i\sqrt{2},$$
$$\sum_{\mu=\pm1} \mu\, h_\mu = -h_- + h_+ = -\sqrt{2},$$
$$\sum_{\alpha=1,2} \boldsymbol{\varepsilon}^{(\alpha),*} = h_{-1}\xi^*_{-1} + h_{+1}\xi^*_{+1}. \tag{33}$$

G. Case of $l_i = 0, l_f = 1, l_\gamma = 1$

In the case of $l_i = 0$, $l_f = 1$, $l_\gamma = 1$ integrals (28) are simplified to [see Appendix B, Eqs. (B22)]

$$\mathbf{I}_1 = -i\sqrt{\frac{3\pi}{2}} \sum_{\mu=\pm1} \boldsymbol{\xi}_\mu\, \mu \times \left[p^M_{l_\gamma=1,\,\mu} - i\mu\, p^E_{l_\gamma=1,\,\mu}\right],$$
$$I_2 = -i\sqrt{\frac{3\pi}{2}} \sum_{\mu=\pm1} \left[\mu\, \tilde{p}^M_{l_\gamma=1,\,\mu} - i\, \tilde{p}^E_{l_\gamma=1,\,\mu}\right], \tag{34}$$

where matrix elements are simplified to [see details in Appendix B, Eqs. (B25)]

$$p^M_{l_\gamma\mu} = 0,$$
$$p^E_{l_\gamma\mu} = \frac{1}{6}\sqrt{\frac{1}{\pi}} J_1(0,1,0) - \frac{47}{240}\sqrt{\frac{1}{2\pi}} J_1(0,1,2),$$
$$\tilde{p}^M_{1\mu}(c) = \frac{\mu}{2\sqrt{2\pi}} \tilde{J}(c,0,1,1), \quad \tilde{p}^E_{1\mu}(c) = 0. \tag{35}$$

We substitute these solutions into Eq. (34) and obtain [see Appendix B, Eqs. (B25) and (B26)]:

$$\mathbf{I}_1 = -\frac{1}{6}\sqrt{\frac{3}{2}} \sum_{\mu=\pm1} \boldsymbol{\xi}_\mu \left(J_1(0,1,0) - \frac{47}{40}\sqrt{\frac{1}{2}} J_1(0,1,2)\right). \tag{36}$$

Integrals do not depend on vectors of polarization. So, we simplify further:

$$\mathbf{I}_1 = -\frac{1}{6}\sqrt{\frac{3}{2}} \left(J_1(0,1,0) - \frac{47}{40}\sqrt{\frac{1}{2}} J_1(0,1,2)\right) (\boldsymbol{\xi}_{\mu=+1} + \boldsymbol{\xi}_{\mu=-1}). \tag{37}$$

Also from Eqs. (34) we find

$$I_2(\alpha) = -i\,\frac{\sqrt{3}}{2}\,\tilde{J}(\alpha,0,1,1). \tag{38}$$

H. Action on vectors of polarization

Now we calculate the summation over vectors of polarization. We use the definition of vectors of polarizations as in Eqs. (57) and (58) in Ref. [28] (see Appendix C in that paper for details):

$$\boldsymbol{\varepsilon}^{(1)} = \frac{1}{\sqrt{2}}(\boldsymbol{\xi}_{-1} - \boldsymbol{\xi}_{+1}), \quad \boldsymbol{\varepsilon}^{(2)} = \frac{i}{\sqrt{2}}(\boldsymbol{\xi}_{-1} + \boldsymbol{\xi}_{+1}), \tag{39}$$

and

$$\boldsymbol{\varepsilon}^{(1)} \cdot (\boldsymbol{\xi}_{\mu=+1} + \boldsymbol{\xi}_{\mu=-1}) = 0, \quad \boldsymbol{\varepsilon}^{(2)} \cdot (\boldsymbol{\xi}_{\mu=+1} + \boldsymbol{\xi}_{\mu=-1}) = -i\sqrt{2}. \tag{40}$$

On such a basis, from Eq. (37) we find

$$\boldsymbol{\varepsilon}^{(1)} \cdot \mathbf{I}_1 = 0, \quad \boldsymbol{\varepsilon}^{(2)} \cdot \mathbf{I}_1(\alpha) = i\,\frac{\sqrt{3}}{6} \cdot \left(J_1(\alpha,0,1,0) - \frac{47}{40}\sqrt{\frac{1}{2}} \cdot J_1(\alpha,0,1,2)\right). \tag{41}$$

Now we can recalculate the matrix element (27) as (at $\mu = 1$ it equals to zero)

$$\left\langle \Psi_{E_f}(\mathbf{r},\mathbf{q}) \right| \hat{H}_\gamma(\mathbf{k}_\gamma, \varepsilon^{(\alpha=2)}) \left| \Psi_{E_i}(\mathbf{r},\mathbf{q}) \right\rangle = \frac{\sqrt{2}\,e\,\hbar^2}{12\,m_N c} \left\{ F_1 \left[J_1\left(-\frac{1}{\sqrt{6}},0,1,0\right) - \frac{47}{40}\sqrt{\frac{1}{2}} J_1\left(-\frac{1}{\sqrt{6}},0,1,2\right)\right] - 2\left[J_1\left(\sqrt{\frac{2}{3}},0,1,0\right) - \frac{47}{40}\sqrt{\frac{1}{2}} J_1\left(\sqrt{\frac{2}{3}},0,1,2\right)\right]\right\}, \tag{42}$$

where integrals are defined in Eqs. (31).

I. Resonating group method

We use the algebraic version of the resonating group method, which was formulated in Refs. [29,30] to study the structure of two- and three-cluster systems. Two main merits (advantages) of the algebraic version of the RGM are (i) it employs a full set of oscillator functions to expand wave functions of relative motion of clusters and, thus, reduces the many-particle Schrödinger equation to a set of linear algebraic equations, and (ii) it implements proper boundary conditions for bound and continuous-spectrum states in discrete, oscillator space.

To solve the Schrödinger equations (10) and (13) for the deuteron and $p+d$ system, wave functions $\phi_{E_d,l}(r)$ and $\psi_{E,L}(q)$ are expanded over the basis of oscillator functions,

$$\phi_{E_d,l}(r) = \sum_{n=0}^{N\max} C_n^{(E_d,l)} \Phi_{nl}(r,b), \tag{43}$$
$$\psi_{E,L}(q) = \sum_{n=0}^{N\max} C_n^{(E,L)} \Phi_{nL}(q,b), \tag{44}$$

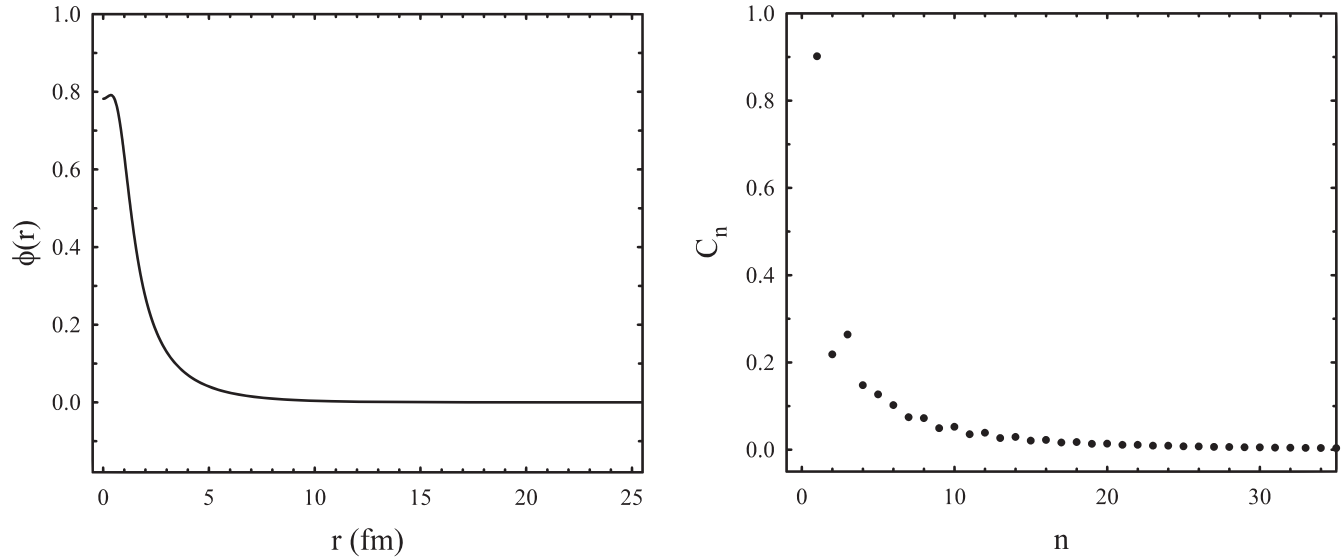

FIG. 2. Wave function of the deuteron in the coordinate space $\phi(r)$ as a function of coordinate r (left panel) and in the oscillator space C_n as a function of n (right panel).

where $\Phi_n(r, b)$ is an oscillator function,

$$\Phi_{nL}(r, b) = (-1)^n N_{nL}\, b^{-3/2} \rho^L e^{-\frac{1}{2}\rho^2} L_n^{L+1/2}(\rho^2),$$
$$\rho = \frac{r}{b}, \tag{45}$$

and b is the oscillator length, and

$$N_{nL} = \sqrt{\frac{2\Gamma(n+1)}{\Gamma(n+L+3/2)}}.$$

A set of expansion coefficients $\{C_n^{(E_d,l)}\}$ can be considered as the deuteron wave function in the oscillator representation, while the expansion coefficients $\{C_n^{(E,L)}\}$ are then the wave functions of relative motion of proton and deuteron in the same representation.

J. Wave function of deuteron

Let us consider the wave function of the deuteron. The wave function of the bound state of the deuteron was obtained with the Minnesota NN potential [33]. This potential creates the bound state at $E_d = -2.202$ MeV, which has to be compared with the experimental value $E_d = -2.225$ MeV. The wave function of the deuteron is shown in Fig. 2 in the coordinate space (left panel) and in the oscillator space (right panel). This wave function was constructed with 200 oscillator functions (N max $= 199$). One can see that only a small number of basis functions ($0 \leqslant n \leqslant 25$) give a noticeable contribution.

In the coordinate representation, the deuteron function has a long exponential tail,

$$\phi_{E_d,L=0}(\mathbf{r}) \approx \exp\{-\kappa r\}/r, \tag{46}$$

where

$$\kappa = \sqrt{\frac{2m|E_d|}{\hbar^2}} = \sqrt{\frac{2 \times 2.202}{41.47}} = 0.325\,879\ \text{fm}^{-1}.$$

In this case, with such a definition of κ, the vector Jacobi r is measured in fm.

It is interesting to note that the function (46) is an exact solution to the two-body problem with the contact interaction

$$V(r) = V_0 \delta(r).$$

This interaction is also called the zero-range interaction and is widely used in atomic and nuclear physics (for more details see Ref. [34]). We will use the normalized-to-unity function

$$\phi(r) = \sqrt{2\kappa}\, \exp\{-\kappa r\}/r, \tag{47}$$

to approximate the correct wave function of the deuteron.

In the shell-model approximation, the wave function of the deuteron bound state is a Gaussian function,

$$\phi(r) = \frac{1}{b^{3/2}} \exp\left\{-\frac{1}{2}\left(\frac{r}{b}\right)^2\right\}. \tag{48}$$

The form factor of the deuteron is then

$$\langle\phi(\mathbf{r})| \exp\left\{-\frac{i}{\sqrt{2}}(\mathbf{k}_\gamma \mathbf{r})\right\} |\phi(\mathbf{r})\rangle = \exp\left\{-\frac{1}{8}(k_\gamma b)^2\right\}. \tag{49}$$

If we take the deuteron wave function in the form

$$\phi(r) = \sqrt{2\kappa}\, \exp\{-\kappa r\}/r, \tag{50}$$

then we obtain the deuteron form factor

$$\langle\phi(\mathbf{r})| \exp\left\{-\frac{i}{\sqrt{2}}(\mathbf{k}_\gamma \mathbf{r})\right\} |\phi(\mathbf{r})\rangle = \frac{2\sqrt{2}\kappa}{k_\gamma} \arctan\left(\frac{k_\gamma}{2\sqrt{2}\kappa}\right). \tag{51}$$

The form factor from Eq. (51) as a function of k_γ demonstrates a slower decrease compared to the form factor of the shell mode (49).

K. Matrix elements in the folding approximation

The matrix element of bremsstrahlung emission of photons for two s clusters (i.e., for clusters with $1 \leqslant A_\alpha \leqslant 4$ or for n, p, d, ^{3}H, ^{3}He, ^{4}He) can be written down as (see Ref. [28], for details)

$$\left\langle \Psi_{E_f l_f} \middle| \hat{H}_\gamma(\mathbf{k}_\gamma, \boldsymbol{\varepsilon}^{(\alpha)}) \middle| \Psi_{E_i l_i} \right\rangle_{\text{fold}} = \frac{e\hbar}{m_N c} \left\{ \sqrt{\frac{A_2}{A_1 A}} \left\langle R_{E_f l_f}(r)\, Y_{l_f m_f}(\widehat{\mathbf{r}}_i) \right| \exp -i \sqrt{\frac{A_2}{A_1 A}}\, (\mathbf{k}_\gamma, \mathbf{r})\, (\boldsymbol{\varepsilon}^{(\alpha)}, \hat{\boldsymbol{\pi}}) \left| R_{E_i l_i}(r)\, Y_{l_i m_i}(\widehat{\mathbf{r}}_i) \right\rangle F_1 \right.$$
$$\left. - \sqrt{\frac{A_1}{A_2 A}} \left\langle R_{E_f l_f}(r)\, Y_{l_f m_f}(\widehat{\mathbf{r}}_i) \right| \exp i \sqrt{\frac{A_1}{A_2 A}}\, (\mathbf{k}_\gamma, \mathbf{r})\, (\boldsymbol{\varepsilon}^{(\alpha)}, \hat{\boldsymbol{\pi}}) \left| R_{E_i l_i}(r)\, Y_{l_i m_i}(\widehat{\mathbf{r}}_i) \right\rangle F_2 \right\}. \tag{52}$$

In the standard approximation of the resonating group method, form factor F_n equals ($n = 1, 2$)

$$F_n = \langle \Phi_n(A_n) | F_0^{(n)} | \Phi_n(A_n) \rangle = Z_n \exp -\frac{1}{4} \frac{A_n - 1}{A_n} (k, b)^2, \tag{53}$$

with b as the oscillator length. Using property (24),

$$\left\langle \psi_{E_f}(\mathbf{q}) \right| \exp\{\pm i\, \alpha'\, (\mathbf{k}_\gamma \mathbf{q})\}\, (\varepsilon^{(\alpha)}, \pi^*_{\mathbf{q}}) \left| \psi_{E_i}(\mathbf{q}) \right\rangle = i\hbar\, \varepsilon^{(\alpha)}\, \mathbf{I}_1(\mp\alpha'), \tag{54}$$

the matrix element is rewritten as

$$\left\langle \Psi_{E_f l_f} \middle| \hat{H}_\gamma(\mathbf{k}_\gamma, \varepsilon^{(\alpha)}) \middle| \Psi_{E_i l_i} \right\rangle_{\text{fold}} = i\, \frac{e\hbar^2}{m_N c}\, \varepsilon^{(\alpha)} \left\{ \sqrt{\frac{A_2}{A_1 A}} \mathbf{I}_1\left(\sqrt{\frac{A_2}{A_1 A}} \right) F_1 - \sqrt{\frac{A_1}{A_2 A}} \mathbf{I}_1\left(-\sqrt{\frac{A_1}{A_2 A}} \right) F_2 \right\}. \tag{55}$$

Now we take into account property (41),

$$\boldsymbol{\varepsilon}^{(1)} \cdot \mathbf{I}_1 = 0, \quad \boldsymbol{\varepsilon}^{(2)} \cdot \mathbf{I}_1(\alpha) = i\, \frac{\sqrt{3}}{6} \cdot \left(J_1(\alpha, 0, 1, 0) - \frac{47}{40} \sqrt{\frac{1}{2}} \cdot J_1(\alpha, 0, 1, 2) \right),$$

and obtain

$$\left\langle \Psi_{E_f l_f} \middle| \hat{H}_\gamma(\mathbf{k}_\gamma, \varepsilon^{(\alpha)}) \middle| \Psi_{E_i l_i} \right\rangle_{\text{fold}} = \frac{\sqrt{3}\, e\hbar^2}{6\, m_N c} \left\{ \sqrt{\frac{A_2}{A_1 A}} \left[J_1\left(\sqrt{\frac{A_2}{A_1 A}},\, 0, 1, 0 \right) - \frac{47}{40} \sqrt{\frac{1}{2}}\, J_1\left(\sqrt{\frac{A_2}{A_1 A}},\, 0, 1, 2 \right) \right] F_1 \right.$$
$$\left. - \sqrt{\frac{A_1}{A_2 A}} \left[J_1\left(-\sqrt{\frac{A_1}{A_2 A}},\, 0, 1, 0 \right) - \frac{47}{40} \sqrt{\frac{1}{2}}\, J_1\left(-\sqrt{\frac{A_1}{A_2 A}},\, 0, 1, 2 \right) \right] F_2 \right\}. \tag{56}$$

In particular, for proton-deuteron scattering we have (we choose the first index for the proton: $A_1 = 1$, $F_1 = F_{\text{p}}$; the second index for the deuteron: $A_2 = 2$, $F_2 = F_{\text{D}}$)

$$\left\langle \Psi_{E_f l_f} \middle| \hat{H}_\gamma(\mathbf{k}_\gamma, \varepsilon^{(\alpha)}) \middle| \Psi_{E_i l_i} \right\rangle_{\text{fold}} = \frac{\sqrt{3}\, e\hbar^2}{6\, m_N c} \left\{ \sqrt{\frac{2}{3}} \left[J_1\left(\sqrt{\frac{2}{3}},\, 0, 1, 0 \right) - \frac{47}{40} \sqrt{\frac{1}{2}}\, J_1\left(\sqrt{\frac{2}{3}},\, 0, 1, 2 \right) \right] F_{\text{p}} \right.$$
$$\left. - \sqrt{\frac{1}{6}} \left[J_1\left(-\sqrt{\frac{1}{6}},\, 0, 1, 0 \right) - \frac{47}{40} \sqrt{\frac{1}{2}}\, J_1\left(-\sqrt{\frac{1}{6}},\, 0, 1, 2 \right) \right] F_{\text{D}} \right\}. \tag{57}$$

For further analysis it is more convenient to rewrite this solution as

$$\left\langle \Psi_{E_f l_f} \middle| \hat{H}_\gamma(\mathbf{k}_\gamma, \varepsilon^{(\alpha)}) \middle| \Psi_{E_i l_i} \right\rangle_{\text{fold}} = \frac{\sqrt{2}\, e\hbar^2}{12\, m_N c} \left\{ \left[J_1\left(-\sqrt{\frac{1}{6}},\, 0, 1, 0 \right) - \frac{47}{40} \sqrt{\frac{1}{2}}\, J_1\left(-\sqrt{\frac{1}{6}},\, 0, 1, 2 \right) \right] F_{\text{D}} \right.$$
$$\left. - 2 \left[J_1\left(\sqrt{\frac{2}{3}},\, 0, 1, 0 \right) - \frac{47}{40} \sqrt{\frac{1}{2}}\, J_1\left(\sqrt{\frac{2}{3}},\, 0, 1, 2 \right) \right] F_{\text{p}} \right\}. \tag{58}$$

L. Definition of the cross section of bremsstrahlung emission of photons and resulting formulas

The cross-section of bremsstrahlung emission of photons is [28]

$$\frac{d\,\sigma^{(1)}}{d\Omega_{A_1}\, d\Omega_{A_2}\, d\Omega_\gamma} = \frac{E_\gamma}{(2\pi\hbar)^4} \left(\frac{p_{1f}}{\hbar c} \right) \frac{\sin^2\theta_1\, \sin^2\theta_2}{sin^5(\theta_1 + \theta_2)} \times \frac{1}{2J+1} \sum_{\mu M_i} |\langle \Psi_{\tilde{E}\tilde{L}} | \hat{H}_\gamma(\mathbf{k}_\gamma, \varepsilon^{(\alpha)}) | \Psi_{EL} \rangle|^2, \tag{59}$$

where p_1 is the momentum of the incident nucleus (cluster) A_1, and θ_1 and θ_2 are scattering angles of the first and second clusters in the laboratory frame.

We write down the final formulas of matrix elements of bremsstrahlung emission in the proton-deuteron scattering. It turns out that in the first approach [we will call it the *three-cluster model*; see Eq. (27)] and in the second approach [we will call it the *folding model*; see Eq. (58)] matrix elements are the same:

$$\left\langle \Psi_{E_f}(\mathbf{r},\mathbf{q})\right| \hat{H}_\gamma(\mathbf{k}_\gamma,\varepsilon^{(\alpha=2)})\left|\Psi_{E_i}(\mathbf{r},\mathbf{q})\right\rangle = \frac{\sqrt{2}\,e\,\hbar^2}{12\,m_N c}\left\{\left[J_1\left(-\frac{1}{\sqrt{6}},0,1,0\right)-\frac{47}{40}\sqrt{\frac{1}{2}}\cdot J_1\left(-\frac{1}{\sqrt{6}},0,1,2\right)\right]F_1 - 2\left[J_1\left(\sqrt{\frac{2}{3}},0,1,0\right)-\frac{47}{40}\sqrt{\frac{1}{2}}\cdot J_1\left(\sqrt{\frac{2}{3}},0,1,2\right)\right]\right\}. \tag{60}$$

The integrals are [see Eqs. (31)]

$$J_1(\alpha,l_i,l_f,n)=\int_0^{+\infty}\frac{dR_i(r,l_i)}{dr}\,R_f^*(l_f,r)\,j_n(\alpha\,k_\gamma r)\,r^2dr. \tag{61}$$

III. ANALYSIS, NUMERICAL CALCULATIONS

To understand the role of the deuteron structure, we are going to perform three (four) types of calculations. They are distinguished by the wave function of the deuteron and are labeled by indexes 0 (C), S, and R. The index 0 means that the deuteron is considered a structureless particle and, thus, its internal structure is ignored. [If the wave function of the deuteron is approximated by the case of the contact interaction (47), we will use the index C]. The index S stands for the shell-model approximation (48) of the wave function of deuteron, and the last case R means that the realistic wave function (44) of the deuteron is involved in calculations.

A. Deuteron wave functions and form factor

The key element of our model is the wave function of the deuteron bound state. This function will determine the interaction of the proton and deuteron. Thus we start our analysis from deuteron wave functions in different models and approximations. In Figs. 3 and 4 we display wave functions of deuteron obtained with the Minnesota potential. The shell model (SM) and cluster model (CM) visually are very similar. However, displaying wave functions on a logarithmic scale, we see that they have quite different asymptotic behavior. Deuteron form factors calculated within the shell model and cluster model are shown in Figs. 5 and 6. If the zero-range interaction is used to determine the wave function of the deuteron (47), then the deuteron form factor is

$$F_1(k_\gamma)=\frac{2\sqrt{2}\kappa}{k_\gamma}\arctan\left(\frac{k_\gamma}{2\sqrt{2}\kappa}\right). \tag{62}$$

B. Wave functions of the $p+d$ system

In Fig. 7 we display phase shifts of the elastic $p+d$ scattering. One can see that the strongest interaction is observed in the $1/2^+$ state, where the nucleus ^{3}He has a bound state. For energy $E>100$ MeV, all displayed phase shifts are very close to zero. This is an additional indication that the potential of the $p+d$ interaction is weak and that the Born approximation can be used for this energy range.

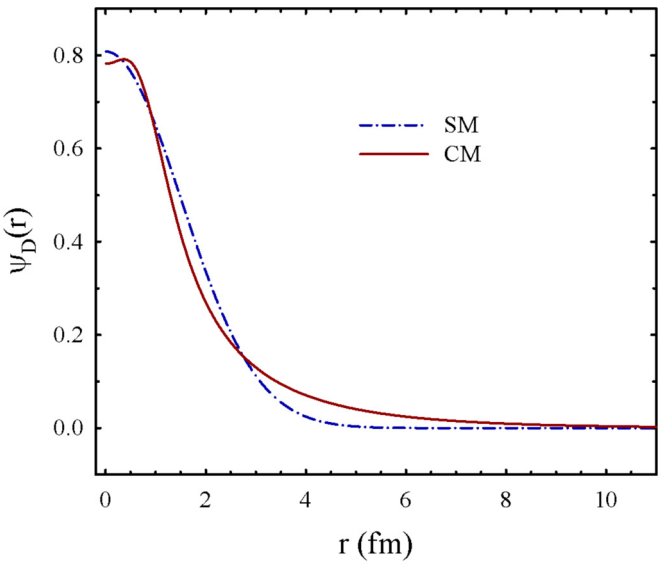

FIG. 3. Wave functions of the deuteron obtained in the shell model (SM) and cluster model (CM).

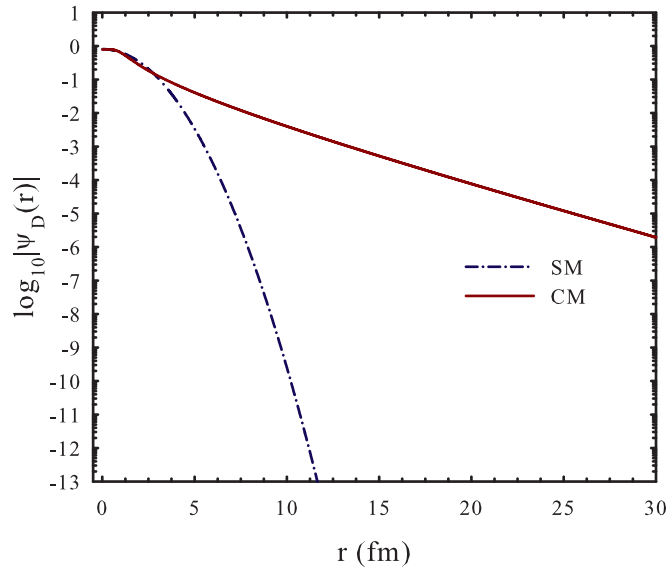

FIG. 4. Asymptotic form of the deuteron wave functions constructed in the shell model (SM) and cluster model (CM) (the logarithm of the wave function with base of 10 is used on the vertical axis).

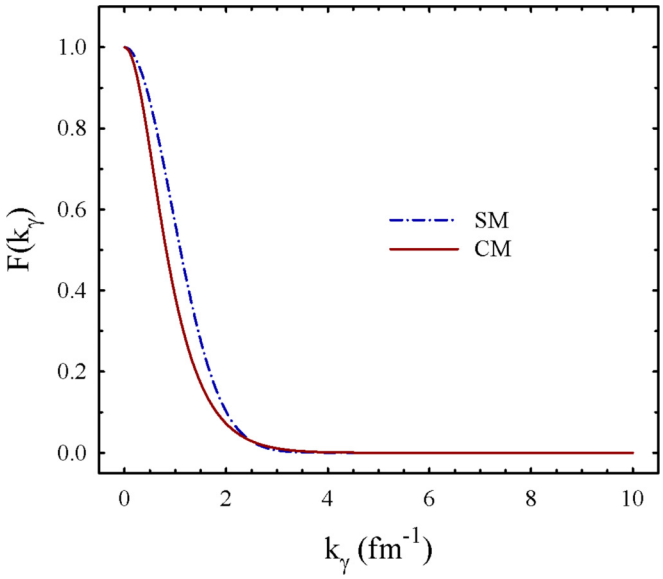

FIG. 5. Form factors of the deuteron determined in the shell and cluster models.

We constructed wave functions of the continuous spectrum states using the diagonalization procedure of the 100×100 matrix of Hamiltonian. Details and justification of this procedure can be found, for example, in Refs. [35,36]. Figure 8 shows wave functions of $1/2^+$ states as a function of the distance between the proton and deuteron. In Fig. 9 we display wave functions for the $1/2^-$ state. Note that the states $1/2^+$ and $1/2^-$ can be connected by the dipole transition operator. General features of the displayed wave functions are that they have large amplitude at relatively small distances between clusters ($r < 5$ fm) and that they slowly decrease as $1/r$.

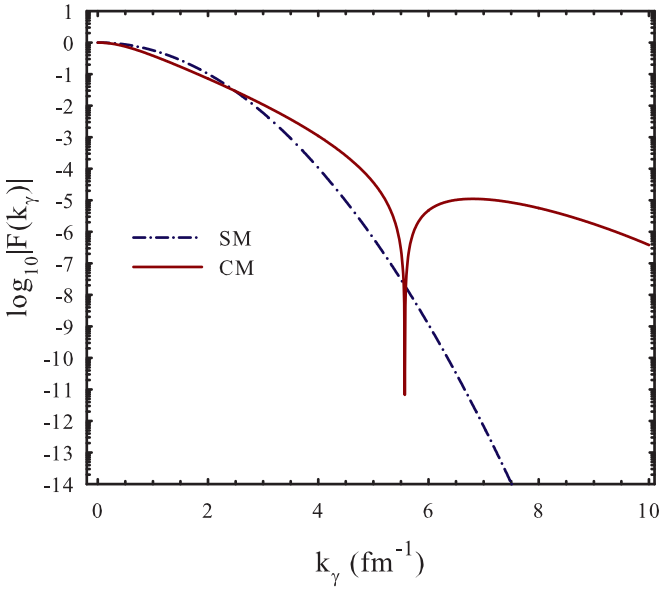

FIG. 6. Form factors of the deuteron in logarithmic scale calculated in the shell and cluster models (the logarithm of the wave function with base of 10 is used on the vertical axis).

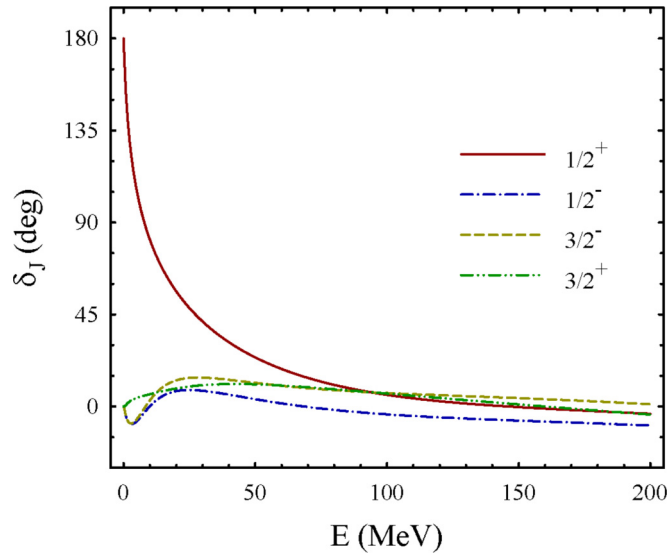

FIG. 7. Phase shifts of the elastic $p + d$ scattering.

C. Different *NN* potentials

In this section we consider how the shape of nucleon-nucleon potential affects phase shifts of the elastic $p + d$ scattering. For this aim, we were involved in our calculations of two new *NN* potentials. They are the Volkov potential (VP) [37] and modified Hasegawa-Nagata potential (MHNP) [38,39]. These potentials alongside with the Minnesota potential (MP) are often used in different cluster models. It is demonstrated in Fig. 10, where the even components V_{31} and V_{13} of three nucleon-nucleon potentials are displayed, that the MHNP has the largest repulsive core at a small distance between nucleons, the VP has the smallest repulsive core,

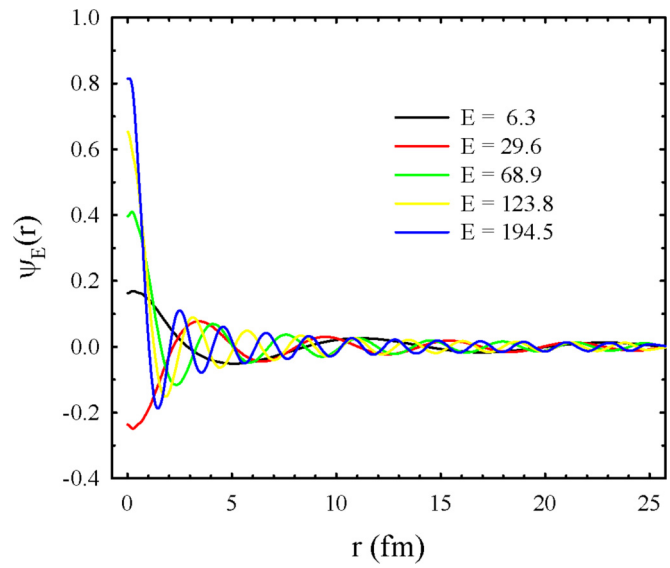

FIG. 8. Wave functions of continuous spectrum states in the $1/2^+$ state of the $p + d$ system (on the vertical axis the wave function is in units of fm$^{-3/2}$).

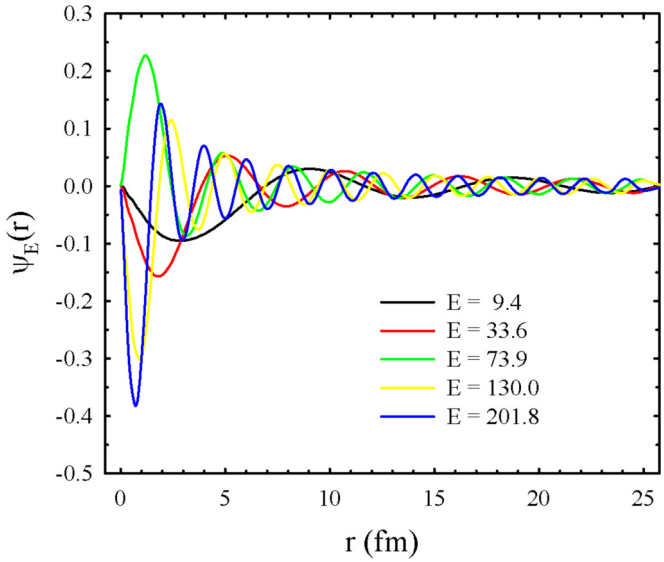

FIG. 9. Wave functions of relative motion of the proton with respect to the deuteron in the $1/2^-$ state (on the vertical axis the wave function is in units of fm$^{-3/2}$).

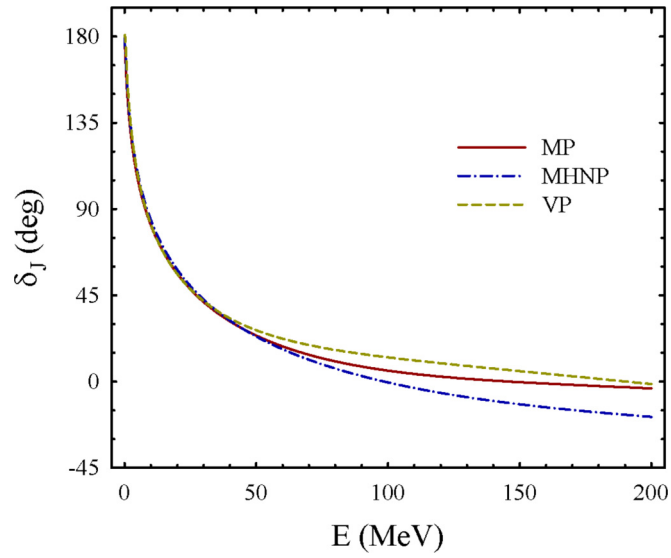

FIG. 11. Phase shifts of the $p+d$ scattering in the $1/2^+$ state calculated with three nucleon-nucleon potentials.

and the MP represents intermediate case among three selected potentials.

In Fig. 11 we display phase shifts of the elastic $p+d$ scattering in the $1/2^+$ state. We can see that the phase shifts slightly depending on the shape of the nucleon-nucleon potentials especially at the energy region $E < 50$ MeV. In the energy range $150 < E < 200$, differences of phase shifts for different potentials are less than 20 degrees.

As a results, wave functions of the elastic $p+d$ scattering obtained with different NN potentials are very close to one another. In Fig. 12 we display wave functions of the $p+d$ system for the energy 147 MeV. The noticeable difference in wave functions is observed at small distances $r < 1$ fm.

Let us consider the $1/2^-$ states in ^{3}He and in the $p+d$ elastic scattering. The $1/2^-$ states can be connected to the $1/2^+$ states by the dipole transition operator. In Fig. 13 we display phase shifts of $p+d$ elastic scattering in the $1/2^-$ states, calculated with three nucleon-nucleon potentials. At low energy ranges, phase shifts exhibit resonance-like behavior, when phase shifts rapidly grow with increasing of energy E. However, the amplitudes of growing are small, besides we estimate that the widths of such resonance states are larger than 20 MeV and their energies are less than 8 MeV. Thus, such states cannot be considered as resonance states.

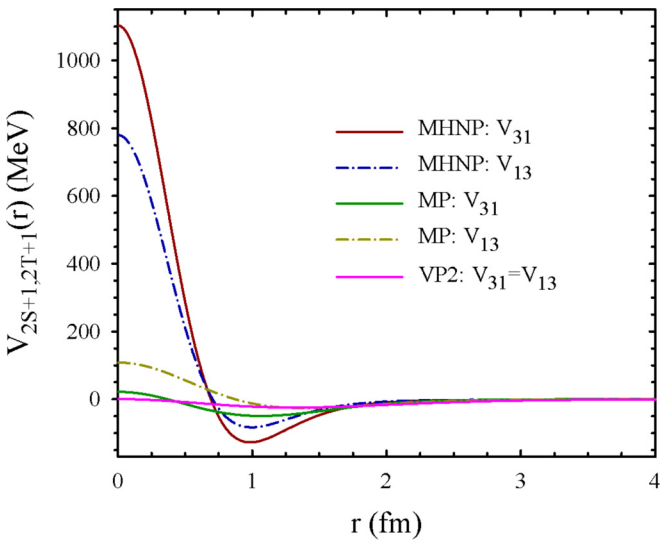

FIG. 10. The even components V_{31} and V_{13} of the MHNP, MP, and VP nucleon-nucleon potentials as a function of the distance between nucleons.

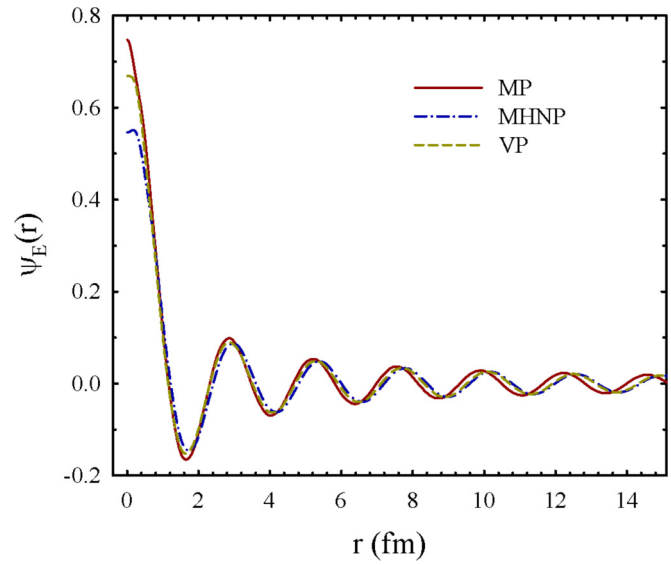

FIG. 12. Wave functions of the $p+d$ system at energy 147 MeV obtained with three different nucleon-nucleon potentials.

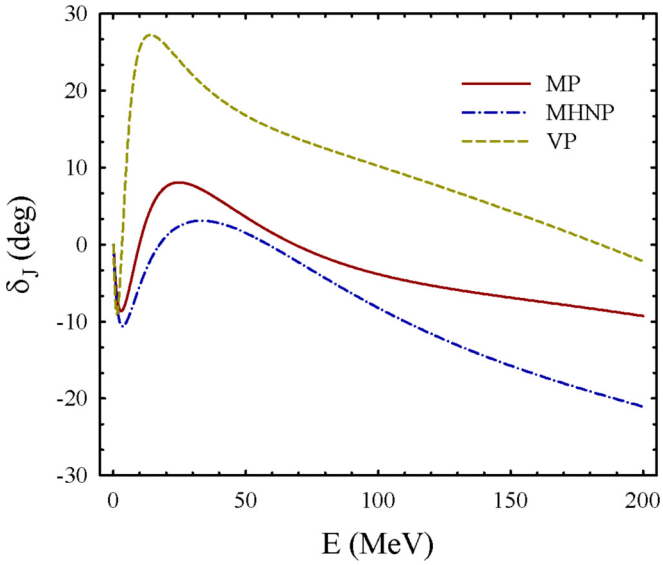

FIG. 13. Phase shifts of the elastic $p+d$ scattering in the $1/2^-$ state obtained with the MP, MHNP, and VP.

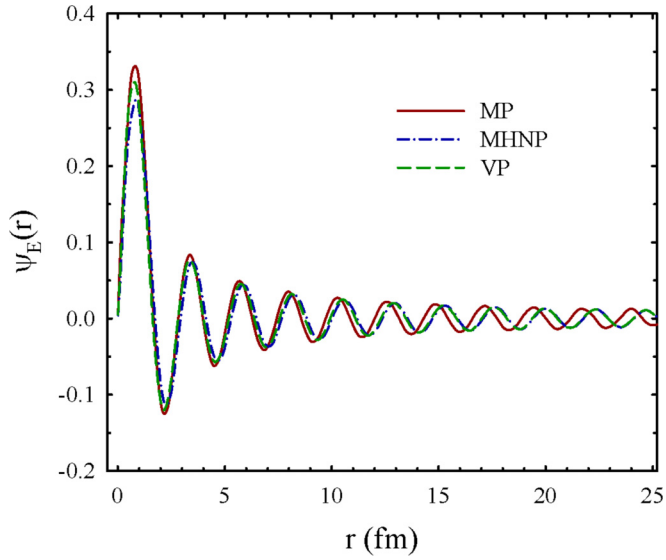

FIG. 15. Wave functions of relative motion of proton and deuteron with energy $E = 147$ MeV and the total angular momentum $J^\pi = 1/2^-$.

This conclusion can be partially confirmed by the behavior of wave functions in the $1/2^-$ states. In Fig. 14 we display wave functions obtained with three nucleon-nucleon potentials at the energy $E = 12.7$ MeV, and in Fig. 15 we show wave functions for a larger value of the energy, $E = 147$ MeV. As we can see, the wave functions at relatively small and large energies have noticeable maxima at relatively small distances ($0.8 < r < 2.5$ fm) between the proton and deuteron. We may conclude that maxima of wave functions in the $1/2^-$ state at small distances are due to the interplay between effects of nucleon-nucleon and Coulomb interactions from one side and effects of the Pauli principle from another side.

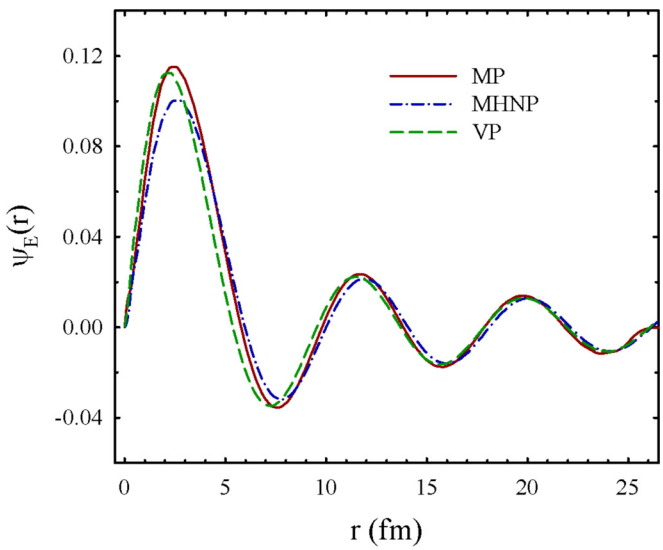

FIG. 14. Wave functions of relative motion of proton and deuteron with energy $E = 12.7$ MeV and the total angular momentum $J^\pi = 1/2^-$.

D. Dependence of the bremsstrahlung cross section on the structure of deuteron

We are interested in the question, is the bremsstrahlung cross section dependent on the structure of the deuteron? In the previous section we discussed several forms of the deuteron wave functions. Two of them are presented in analytic form, and one of them is obtained numerically by solving the two-body Schrödinger equation with the Minnesota potential. The deuteron wave function of the oscillator shell model, displayed in Eq. (48), allows us in a simple way to study the effects of the deuteron structure on the bremsstrahlung cross section. Indeed, this wave function depends on the oscillator length b. Recall, that the oscillator length is selected to minimize the ground state energy of the deuteron with a selected potential. If in Eq. (48) we put $b = 0$, then we obtain a structureless deuteron or, in other words, we disregard of the internal structure of the deuteron.

The oscillator length b can be considered the variational parameter in our two-cluster model. An optimal value of b can be determined by comparing the theoretical and experimental data at different energies of protons colliding with deuterons. Variation of the oscillator length allows us to demonstrate clearly how strongly the bremsstrahlung cross sections depends on the shape of the deuteron wave function.

Some information about the structure of the deuteron is included in its form factor, which is presented in the folding and cluster approaches. The matrix element of bremsstrahlung emission in both approaches is defined by Eq. (60) as ($F_p = 1$), where we will consider the form factor of the deuteron in the folding approach given by Eq. (53) ($Z_D = 1$, $A_D = 2$ for the deuteron),

$$F_D(k_\gamma) = Z_D \exp -\frac{1}{4}\frac{A_D - 1}{A_D}(k_\gamma b)^2 = \exp -\frac{1}{8}(k_\gamma b)^2 \quad (63)$$

with the oscillator length b.

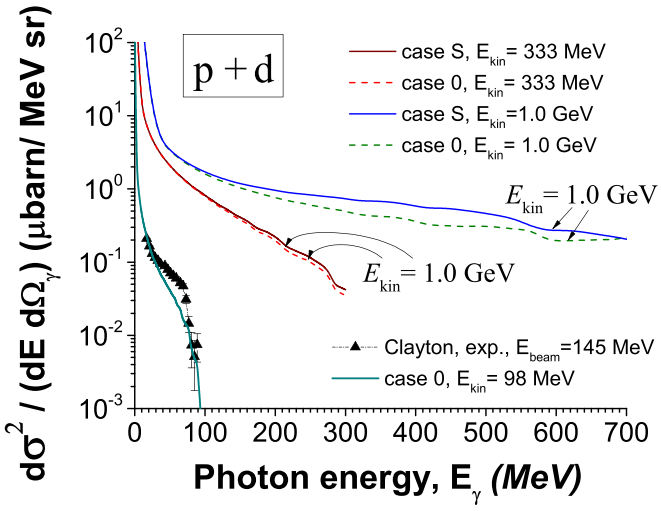

FIG. 16. Cross sections of bremsstrahlung emission for $p + d$ (in the experiment [40] the deuteron is the projectile and the proton is the target) with the included structure of the deuteron and without it calculated at deuteron beam energies of 145 MeV ($E_{\rm kin} = 98$ MeV), 500 MeV ($E_{\rm kin} = 333$ MeV), and 1.5 GeV ($E_{\rm kin} = 1.0$ GeV) [Parameters of calculations: cross section is defined in Eq. (59) and then averaged over all angles with the exception of photon emission angle θ used in experiments ($\theta = 60^\circ$; see also Ref. [45], Fig. 5); as nonzero oscillator length for deuteron we choose $b = 1.3$ fm; $R_{\rm max} = 20\,000$ fm and 2 500 000 intervals are used in the numerical integration; time of computer calculations is 2–4 min for 40 points of each calculated spectrum; kinetic energy $E_{\rm kin}$ of relative motion of proton and deuteron is used in calculations of bremsstrahlung matrix elements, and is $E_{\rm kin} = (2/3)E_{\rm beam}$]. Here, experimental data at 145 MeV of beam energy given by black triangles are extracted from Ref. [40]. See also free $pn\gamma$ calculation of Herrmann, Speth, and Nakayama at 150 and 200 MeV in Ref. [41] (see also Fig. 6 in Ref. [40]).

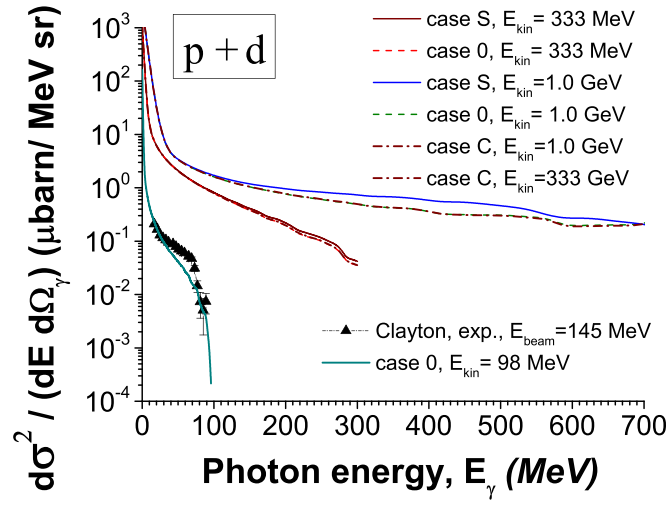

FIG. 17. Cross sections of bremsstrahlung emission for $p + d$ with including the new form factor calculated at beam energies of 145 MeV ($E_{\rm kin} = 98$ MeV), 500 MeV ($E_{\rm kin} = 333$ MeV), and 1.5 GeV ($E_{\rm kin} = 1.0$ GeV) [Parameters of calculations: cross section is defined in Eq. (59); matrix element is defined in Eq. (60); as nonzero oscillator length for the deuteron we choose $b = 1.3$ fm; $R_{\rm max} = 20\,000$ fm and 2 500 000 intervals are used in the numerical integration; time of computer calculations is 2–4 min for 40 points of each calculated spectrum; kinetic energy $E_{\rm kin}$ of relative motion of proton and deuteron is used in calculations of bremsstrahlung matrix elements, and is $E_{\rm kin} = (2/3)E_{\rm beam}$]. Here, experimental data at 145 MeV of beam energy given by black triangles are extracted from Ref. [40].

Results of such calculations at different energies of the beam are presented in Fig. 16. From such results we conclude the following.

(1) The difference between cross sections calculated with the included structure of the deuteron and without it at the same beam energy becomes visible and stable at higher beam energy (higher than 500 MeV).
(2) Calculation with realistic wave functions (including the structure of the deuteron) gives a larger cross section of bremsstrahlung than the cross section without the inclusion of the structure of the deuteron.
(3) In xperiment [40] the beam energy used, 145 MeV, is not effective for such a study (it is demonstrated by cross sections at 1.5 GeV in comparison with the cross section at 145 MeV in this figure). At the same time, possible new measurements of bremsstrahlung cross sections but at higher energies (about 0.5–1.5 GeV of beam energy) will allow us to extract information about the structure of the deuteron (realistic oscillator length and wave function).
(4) More precise information about the structure of the deuteron can be obtained if one organizes unified experiments in the measurement of the bremsstrahlung cross section at two different energies of the beam (for example, at 145 MeV and 500 MeV). Then, our model will estimate the ratio between two bremsstrahlung cross sections at such energies and provide a realistic value of the oscillator length with high precision.

E. Dependence of bremsstrahlung cross section on the new form factor of the deuteron

Now we will analyze how much the spectrum is changed if one uses the new form factor of the deuteron instead of previous calculations. So, we have the matrix element in the form (60) with the form factor of the deuteron given by Eq. (62). Note that this form factor of the deuteron does not include the oscillator length. Results of such calculations with the new form factor are presented in Fig. 17. From these calculations one can see that the inclusion of the new form factor reduces the full cross section a little. But, general dependence of the cross section on this form of form factor is observed at higher energies.

IV. CONCLUSIONS AND PERSPECTIVES

In this paper, we investigated the emission of bremsstrahlung photons in the scattering of protons off deuterons on the full cluster basis in a wide region of the beam energy from low energies to 1.5 GeV. To realize these

investigations, we developed a new model. Based on such a model we obtain the following results:

(i) It is demonstrated that the matrix elements of bremsstrahlung emission in the deuteron-proton scattering in the three-cluster formalism coincides with the corresponding matrix elements in the folding approximation given in Ref. [28].

(ii) The formalism of the model includes the form factor of a deuteron which affects the behavior of bremsstrahlung cross sections and reflects the structure of thedeuteron and the influence of parameters of nucleon-nucleon interactions. This gives the possibility to investigate the structure of nuclei and properties of interactions from analysis of bremsstrahlung cross sections.

(iii) We studied the dependence of the bremsstrahlung cross section on the structure of the deuteron. We find that the oscillator length b, related to the shell-model description of the deuteron, is a convenient parameter for such a study. Analysis of the dependence of the cross section on such a parameter shows the following. At beam energies used in the experiment [40] the cross section is not sensitive enough to variations of oscillator length, i.e., on the internal structure of the deuteron. However, stable differences between cross sections calculated at zero and nonzero oscillator lengths at the same beam energy are observed at higher beam energy (higher than 500 MeV). The spectrum of photons is increased by increasing of the oscillator length inside the full energy region of the emitted photons. However, using the new the deuteron form factor in the cluster formalism [see Eq. (62)] reduces the bremsstrahlung cross section a little.

(iv) We can obtain more precise information about the structure of the deuteron by performing new unified experiments for measurements of the bremsstrahlung cross section at two different energies of the beam (for example, at 145 and 500 MeV or above). Then, our model will estimate the ratio between two bremsstrahlung cross sections at such energies and provide information about the realistic value of the oscillator length with high precision, or, in other words, about the wave function of the deuteron.

We see that the formalism of our model provides a strict basis for the description of the deuteron-proton scattering and emission of virtual photons in the study of dilepton production in deuteron-proton scattering (see, for example, Refs. [41–43]). This can be interesting for further investigations and applications.

ACKNOWLEDGMENTS

We thank Prof. G. Wolf for fruitful discussions concerning different aspects of nuclear collisions at high energies, and Dr. S. A. Omelchenko for fruitful discussions concerning aspects of different nuclear models for scattering and decays. This work was supported in part by the Program of Fundamental Research of the Physics and Astronomy Department of the National Academy of Sciences of Ukraine (Projects No. 0117U000239 and No. 0122U000889). S.P.M. is thankful for support via OTKA Grant No. K138277. V.S.V. is grateful to the Simons foundation for financial support (Award No. 1030284).

APPENDIX A: CALCULATION OF OPERATOR OF BREMSSTRAHLUNG EMISSION IN THREE-CLUSTER MODEL

In this Appendix we will calculate the operator of the emission of bremsstrahlung photons in the three-cluster formalism. We fix the position of nucleons. We assume that vector $\mathbf{r}$ measures the distance between the proton and neutron which form a deuteron. We also assume that $\mathbf{r}_1$ is the coordinate of the first proton and $\mathbf{r}_2$ is the coordinate of the neutron. Vector $\mathbf{r}_3$ determines the location of the second proton. Starting from Eq. (1), this operator is obtained in the following form:

$$\begin{aligned}
\widehat{H}_e(\mathbf{k}_\gamma, \varepsilon^{(\alpha)}) &= \frac{1}{2}\frac{e\hbar}{m_N c}[\widehat{\pi}_1^* \mathbf{A}^*(1) + \mathbf{A}^*(1)\widehat{\pi}_1^* + \widehat{\pi}_3^* \mathbf{A}^*(3) + \mathbf{A}^*(3)\widehat{\pi}_3^*] \\
&= \frac{1}{2}\frac{e\hbar}{m_N c}\{\widehat{\pi}_1^* \varepsilon^{(\alpha)} \exp\{-i(\mathbf{k}_\gamma \rho_1)\} + \varepsilon^{(\alpha)} \exp\{-i(\mathbf{k}_\gamma \rho_1)\}\widehat{\pi}_1^* + \widehat{\pi}_3^* \varepsilon^{(\alpha)} \exp\{-i(\mathbf{k}_\gamma \rho_3)\} + \varepsilon^{(\alpha)} \exp\{-i(\mathbf{k}_\gamma \rho_3)\}\widehat{\pi}_3^*\} \\
&= \frac{1}{2}\frac{e\hbar}{m_N c}\left[(\varepsilon^{(\alpha)}\widehat{\pi}_1^*) \exp\left\{-i\frac{1}{\sqrt{2}}(\mathbf{k}_\gamma \mathbf{r}) + i\frac{1}{\sqrt{6}}(\mathbf{k}_\gamma \mathbf{q})\right\} + \exp\left\{-i\frac{1}{\sqrt{2}}(\mathbf{k}_\gamma \mathbf{r}) + i\frac{1}{\sqrt{6}}(\mathbf{k}_\gamma \mathbf{q})\right\}(\varepsilon^{(\alpha)}\widehat{\pi}_1^*)\right. \\
&\quad \left. + (\varepsilon^{(\alpha)}\widehat{\pi}_3^*) \exp\left\{-i\sqrt{\frac{2}{3}}(\mathbf{k}_\gamma \mathbf{q})\right\} + \exp\left\{-i\sqrt{\frac{2}{3}}(\mathbf{k}_\gamma \mathbf{q})\right\}(\varepsilon^{(\alpha)}\widehat{\pi}_3^*)\right]
\end{aligned}$$

and then

$$\begin{aligned}
\widehat{H}_e(\mathbf{k}_\gamma, \varepsilon^{(\alpha)}) = \frac{1}{2}\frac{e\hbar}{m_N c}\Bigg[&\left(\varepsilon^{(\alpha)}, \frac{1}{\sqrt{2}}\pi_{\mathbf{r}}^* - \frac{1}{\sqrt{6}}\pi_{\mathbf{q}}^*\right) \exp\left\{-i\frac{1}{\sqrt{2}}(\mathbf{k}_\gamma \mathbf{r}) + i\frac{1}{\sqrt{6}}(\mathbf{k}_\gamma \mathbf{q})\right\} + \exp\left\{-i\frac{1}{\sqrt{2}}(\mathbf{k}_\gamma \mathbf{r}) + i\frac{1}{\sqrt{6}}(\mathbf{k}_\gamma \mathbf{q})\right\} \\
&\times \left(\varepsilon^{(\alpha)}, \frac{1}{\sqrt{2}}\pi_{\mathbf{r}}^* - \frac{1}{\sqrt{6}}\pi_{\mathbf{q}}^*\right) + \sqrt{\frac{2}{3}}(\varepsilon^{(\alpha)}\pi_{\mathbf{q}}^*) \exp\left\{-i\sqrt{\frac{2}{3}}(\mathbf{k}_\gamma \mathbf{q})\right\} + \sqrt{\frac{2}{3}} \exp\left\{-i\sqrt{\frac{2}{3}}(\mathbf{k}_\gamma \mathbf{q})\right\}(\varepsilon^{(\alpha)}\pi_{\mathbf{q}}^*)\Bigg].
\end{aligned}$$

Collecting similar terms, we obtain

$$\widehat{H}_e(\mathbf{k}_\gamma, \varepsilon^{(\alpha)}) = \frac{1}{2}\frac{e\hbar}{m_N c}\left[\frac{2}{3}(\varepsilon^{(\alpha)}, \mathbf{k}_\gamma)\exp\left\{-i\frac{1}{\sqrt{2}}(\mathbf{k}_\gamma \mathbf{r}) + i\frac{1}{\sqrt{6}}(\mathbf{k}_\gamma \mathbf{q})\right\} + \frac{2}{3}(\varepsilon^{(\alpha)}\mathbf{k}_\gamma)\exp\left\{-i\sqrt{\frac{2}{3}}(\mathbf{k}_\gamma \mathbf{q})\right\}\right.$$
$$\left. + 2\exp\left\{-i\frac{1}{\sqrt{2}}(\mathbf{k}_\gamma \mathbf{r}) + i\frac{1}{\sqrt{6}}(\mathbf{k}_\gamma \mathbf{q})\right\}\left(\varepsilon^{(\alpha)}, \frac{1}{\sqrt{2}}\pi^*_{\mathbf{r}} - \frac{1}{\sqrt{6}}\pi^*_{\mathbf{q}}\right) + 2\sqrt{\frac{2}{3}}\exp\left\{-i\sqrt{\frac{2}{3}}(\mathbf{k}_\gamma \mathbf{q})\right\}(\varepsilon^{(\alpha)}, \pi^*_{\mathbf{q}})\right].$$

Taking into account that $(\varepsilon^{(\alpha)}, \mathbf{k}_\gamma) = 0$, we obtain

$$\widehat{H}_e(\mathbf{k}_\gamma, \varepsilon^{(\alpha)}) = \frac{1}{2}\frac{e\hbar}{m_N c}\left[\frac{2}{\sqrt{2}}\exp\left\{-i\frac{1}{\sqrt{2}}(\mathbf{k}_\gamma \mathbf{r})\right\}(\varepsilon^{(\alpha)}, \pi^*_{\mathbf{r}})\exp\left\{i\frac{1}{\sqrt{6}}(\mathbf{k}_\gamma \mathbf{q})\right\}\right.$$
$$\left. - \sqrt{\frac{2}{3}}\exp\left\{-i\frac{1}{\sqrt{2}}(\mathbf{k}_\gamma \mathbf{r})\right\}\exp\left\{i\frac{1}{\sqrt{6}}(\mathbf{k}_\gamma \mathbf{q})\right\}(\varepsilon^{(\alpha)}, \pi^*_{\mathbf{q}}) + 2\sqrt{\frac{2}{3}}\exp\left\{-i\sqrt{\frac{2}{3}}(\mathbf{k}_\gamma \mathbf{q})\right\}(\varepsilon^{(\alpha)}, \pi^*_{\mathbf{q}})\right].$$

APPENDIX B: CALCULATIONS OF INTEGRALS

1. A general case

In this Appendix we calculate integrals (21):

$$\mathbf{I}_1 = \langle\, \Phi_f(\mathbf{r}) \,|\, e^{-i\mathbf{k}_\gamma \mathbf{r}}\, \frac{\mathbf{d}}{\mathbf{dr}} |\, \Phi_i(\mathbf{r})\,\rangle_{\mathbf{r}}, \quad I_2 = \langle \Phi_f(\mathbf{r}) \,|\, e^{i c_p \mathbf{k}_\gamma \mathbf{r}} \,|\, \Phi_i(\mathbf{r})\,\rangle_{\mathbf{r}},$$
$$I_3 = \langle \Phi_f(\mathbf{r}) \,|\, e^{-i c_A \mathbf{k}_\gamma \mathbf{r}} \,|\, \Phi_i(\mathbf{r})\,\rangle_{\mathbf{r}}, \quad I_4 = \langle \Phi_f(\mathbf{r}) \,|\, e^{-i c_A \mathbf{k}_\gamma \mathbf{r}}\, V(\mathbf{r}) \,|\, \Phi_i(\mathbf{r})\,\rangle_{\mathbf{r}}. \tag{B1}$$

Here, to two integrals in Eqs. (21) we have added two new types of integrals, which are used in calculations in other problems of bremsstrahlung emission. $V(\mathbf{r})$ is an arbitrary potential function.

We use a multipole expansion of the wave function of photons, following the formalism in Sec. D of Ref. [44] [see Eqs. (29)–(31) and (24)–(28) in that paper]. Here, we obtain the following formulas for matrix elements:

$$\langle k_f |\, e^{-i\mathbf{k}_\gamma \mathbf{r}} \,|\, k_i\rangle_{\mathbf{r}} = \sqrt{\frac{\pi}{2}}\sum_{l_\gamma=1}(-i)^{l_\gamma}\sqrt{2l_\gamma+1}\sum_{\mu=\pm1}\left[\mu\, \tilde{p}^M_{l_\gamma \mu} - i\, \tilde{p}^E_{l_\gamma \mu}\right],$$
$$\langle k_f |\, e^{-i\mathbf{k}_\gamma \mathbf{r}} \frac{\partial}{\partial \mathbf{r}} \,|\, k_i\rangle_{\mathbf{r}} = \sqrt{\frac{\pi}{2}}\sum_{l_\gamma=1}(-i)^{l_\gamma}\sqrt{2l_\gamma+1}\sum_{\mu=\pm1}\boldsymbol{\xi}_\mu\, \mu\, \times \left[p^M_{l_\gamma \mu} - i\mu\, p^E_{l_\gamma \mu}\right]. \tag{B2}$$

We write solutions for integrals based on these formulas (for simplicity, we study the case of $l_i = 0$).

According to the second formula in Eqs. (B2), the first integral is

$$\mathbf{I}_1 = \langle \Phi_f |\, e^{-i\mathbf{k}_\gamma \mathbf{r}} \frac{\partial}{\partial \mathbf{r}} \,|\, \Phi_i\rangle_{\mathbf{r}} = \sqrt{\frac{\pi}{2}}\sum_{l_\gamma=1}(-i)^{l_\gamma}\sqrt{2l_\gamma+1}\sum_{\mu=\pm1}\boldsymbol{\xi}_\mu\, \mu\, \times \left[p^M_{l_\gamma \mu} - i\mu\, p^E_{l_\gamma \mu}\right], \tag{B3}$$

where (see Eqs. (38) at $l_i = 0$ in Ref. [44])

$$p^M_{l_\gamma \mu} = -I_M(0, l_f, l_\gamma, 1, \mu) J_1(0, l_f, l_\gamma),$$
$$p^E_{l_\gamma \mu} = \sqrt{\frac{l_\gamma+1}{2l_\gamma+1}} I_E(0, l_f, l_\gamma, 1, l_\gamma - 1, \mu) J_1(0, l_f, l_\gamma - 1)$$
$$- \sqrt{\frac{l_\gamma}{2l_\gamma+1}} I_E(0, l_f, l_\gamma, 1, l_\gamma + 1, \mu) J_1(0, l_f, l_\gamma + 1) \tag{B4}$$

and (see Eqs. (39) in Ref. [44])

$$J_1(l_i, l_f, n) = \int_0^{+\infty} \frac{dR_i(r, l_i)}{dr}\, R^*_f(l_f, r)\, j_n(k_\gamma r)\, r^2 dr. \tag{B5}$$

For the other integrals from Eqs. (B1) one can get similar solutions [those are directly derived from the first expansion in Eqs. (B2), where the other corresponding radial integrals should be used]:

$$I_2 = \langle \Phi_f \mid e^{i c_p \mathbf{k}_\gamma \mathbf{r}} \mid \Phi_i \rangle_{\mathbf{r}} = \sqrt{\frac{\pi}{2}} \sum_{l_\gamma=1} (-i)^{l_\gamma} \sqrt{2l_\gamma+1} \sum_{\mu=\pm1} \left[\mu\, \tilde{p}^M_{l_\gamma\mu}(-c_p) - i\, \tilde{p}^E_{l_\gamma\mu}(-c_p)\right],$$

$$I_3 = \langle \Phi_f \mid e^{-i c_A \mathbf{k}_\gamma \mathbf{r}} \mid \Phi_i \rangle_{\mathbf{r}} = \sqrt{\frac{\pi}{2}} \sum_{l_\gamma=1} (-i)^{l_\gamma} \sqrt{2l_\gamma+1} \sum_{\mu=\pm1} \left[\mu\, \tilde{p}^M_{l_\gamma\mu}(c_A) - i\, \tilde{p}^E_{l_\gamma\mu}(c_A)\right],$$

$$I_4 = \langle \Phi_f \mid e^{-i c_A \mathbf{k}_\gamma \mathbf{r}} V(\mathbf{r}) \mid \Phi_i \rangle_{\mathbf{r}} = \sqrt{\frac{\pi}{2}} \sum_{l_\gamma=1} (-i)^{l_\gamma} \sqrt{2l_\gamma+1} \sum_{\mu=\pm1} \left[\mu\, \breve{p}^M_{l_\gamma\mu}(c_A) - i\, \breve{p}^E_{l_\gamma\mu}(c_A)\right], \tag{B6}$$

where [see solutions (40) at $l_i = 0$ in Ref. [44] for $\tilde{p}^M_{l_\gamma\mu}$, $\tilde{p}^E_{l_\gamma\mu}$, Eqs. (F14) and (F26) in Ref. [46] for all matrix elements]

$$\begin{aligned}
\tilde{p}^M_{l_\gamma\mu}(c) &= \tilde{I}\,(0, l_f, l_\gamma, l_\gamma, \mu)\tilde{J}\,(c, 0, l_f, l_\gamma),\\
\tilde{p}^E_{l_\gamma\mu}(c) &= \sqrt{\frac{l_\gamma+1}{2l_\gamma+1}}\tilde{I}\,(0, l_f, l_\gamma, l_\gamma-1, \mu)\tilde{J}\,(c, 0, l_f, l_\gamma-1) - \sqrt{\frac{l_\gamma}{2l_\gamma+1}}\tilde{I}\,(0, l_f, l_\gamma, l_\gamma+1, \mu)\tilde{J}\,(c, 0, l_f, l_\gamma+1),\\
\breve{p}^M_{l_\gamma\mu}(c_A) &= \tilde{I}\,(0, l_f, l_\gamma, l_\gamma, \mu)\breve{J}\,(c_A, 0, l_f, l_\gamma),\\
\breve{p}^E_{l_\gamma\mu}(c_A) &= \sqrt{\frac{l_\gamma+1}{2l_\gamma+1}}\tilde{I}\,(0, l_f, l_\gamma, l_\gamma-1, \mu)\breve{J}\,(c_A, 0, l_f, l_\gamma-1) - \sqrt{\frac{l_\gamma}{2l_\gamma+1}}\tilde{I}\,(0, l_f, l_\gamma, l_\gamma+1, \mu)\breve{J}\,(c_A, 0, l_f, l_\gamma+1)
\end{aligned} \tag{B7}$$

and [see solutions (41) in Ref. [44] for $\tilde{J}$ and the corresponding angular integral, Eqs. (F13) and (F21) in Ref. [46] for all matrix elements]

$$\tilde{J}\,(c, l_i, l_f, n) = \int_0^{+\infty} R_i(r)\, R^*_f(l, r)\, j_n(c\, k_\gamma r)\, r^2 dr, \quad \breve{J}\,(c_A, l_i, l_f, n) = \int_0^{+\infty} R_i(r)\, R^*_{l,f}(r)\, V(\mathbf{r})\, j_n(c_A\, kr)\, r^2 dr. \tag{B8}$$

2. Linear and circular polarizations of the photon emitted

We rewrite vectors of *linear* polarization $\boldsymbol{\varepsilon}^{(\alpha)}$ through *vectors of circular polarization* ξ_μ with opposite directions of rotation (see Ref. [32], (2.39), p. 42):

$$\xi_{-1} = \frac{1}{\sqrt{2}}(\boldsymbol{\varepsilon}^{(1)} - i\boldsymbol{\varepsilon}^{(2)}), \quad \xi_{+1} = -\frac{1}{\sqrt{2}}(\boldsymbol{\varepsilon}^{(1)} + i\boldsymbol{\varepsilon}^{(2)}), \quad \xi_0 = \boldsymbol{\varepsilon}^{(3)}. \tag{B9}$$

where

$$h_\pm = \mp\frac{1 \pm i}{\sqrt{2}}, \quad h_{-1} + h_{+1} = -i\sqrt{2}, \quad \sum_{\alpha=1,2} \boldsymbol{\varepsilon}^{(\alpha),*} = h_{-1}\xi^*_{-1} + h_{+1}\xi^*_{+1}. \tag{B10}$$

We have (in Coulomb gauge at $\boldsymbol{\varepsilon}^{(3)} = 0$)

$$\boldsymbol{\varepsilon}^{(1)} = \frac{1}{\sqrt{2}}(\boldsymbol{\xi}_{-1} - \boldsymbol{\xi}_{+1}), \quad \boldsymbol{\varepsilon}^{(2)} = \frac{i}{\sqrt{2}}(\boldsymbol{\xi}_{-1} + \boldsymbol{\xi}_{+1}), \tag{B11}$$

$$\sum_{\mu=\pm1} \xi^*_\mu \cdot \xi_\mu = \frac{1}{2}(\boldsymbol{\varepsilon}^{(1)} - i\boldsymbol{\varepsilon}^{(2)})(\boldsymbol{\varepsilon}^{(1)} - i\boldsymbol{\varepsilon}^{(2)})^* + \frac{1}{2}(\boldsymbol{\varepsilon}^{(1)} + i\boldsymbol{\varepsilon}^{(2)})(\boldsymbol{\varepsilon}^{(1)} + i\boldsymbol{\varepsilon}^{(2)})^* = 2. \tag{B12}$$

Also we will find vectorial products of vectors $\boldsymbol{\xi}_{\pm1}$. From Eqs. (B9) we obtain

$$\boldsymbol{\xi}^*_{-1} = -\boldsymbol{\xi}_{+1}, \quad \boldsymbol{\xi}^*_{+1} = -\boldsymbol{\xi}_{-1}. \tag{B13}$$

From here we obtain vector multiplications as

$$[\boldsymbol{\xi}_{-1} \times \boldsymbol{\xi}_{+1}] = -i\,[\boldsymbol{\varepsilon}^{(1)} \times \boldsymbol{\varepsilon}^{(2)}] = -i\,\boldsymbol{\varepsilon}_z, \tag{B14}$$

$$\begin{aligned}
&[\boldsymbol{\xi}^*_{-1} \times \boldsymbol{\xi}_{+1}] = -[\boldsymbol{\xi}_{+1} \times \boldsymbol{\xi}_{+1}] = 0, \quad [\boldsymbol{\xi}^*_{-1} \times \boldsymbol{\xi}_{-1}] = -[\boldsymbol{\xi}_{+1} \times \boldsymbol{\xi}_{-1}] = i\,\boldsymbol{\varepsilon}_z,\\
&[\boldsymbol{\xi}^*_{+1} \times \boldsymbol{\xi}_{-1}] = -[\boldsymbol{\xi}_{-1} \times \boldsymbol{\xi}_{-1}] = 0, \quad [\boldsymbol{\xi}^*_{+1} \times \boldsymbol{\xi}_{+1}] = -[\boldsymbol{\xi}_{-1} \times \boldsymbol{\xi}_{+1}] = -i\,\boldsymbol{\varepsilon}_z.
\end{aligned} \tag{B15}$$

3. Summation over vectors of polarizations

In this section, we will calculate multiplications of integrals on vectors of polarizations. Let us consider the first integral $\mathbf{I}_1$ which has the form [see Eqs. (B3)]:

$$\mathbf{I}_1 = \langle \Phi_f |\, e^{-i\mathbf{k}_\gamma \mathbf{r}} \frac{\partial}{\partial \mathbf{r}} \,|\, \Phi_i \rangle_{\mathbf{r}} = \sqrt{\frac{\pi}{2}} \sum_{l_\gamma=1} (-i)^{l_\gamma} \sqrt{2l_\gamma+1} \sum_{\mu=\pm1} \boldsymbol{\xi}_\mu \, \mu \, \times \left[p^M_{l_\gamma \mu} - i\mu \, p^E_{l_\gamma \mu} \right]. \tag{B16}$$

We calculate

$$\begin{aligned}
\boldsymbol{\varepsilon}^{(1)} \cdot \mathbf{I}_1 &= -\sqrt{\frac{\pi}{2}} \sum_{l_\gamma=1} (-i)^{l_\gamma} \sqrt{2l_\gamma+1} \, \frac{1}{\sqrt{2}} \sum_{\mu=\pm1} \left[p^M_{l_\gamma \mu} - i \, \mu \, p^E_{l_\gamma \mu} \right], \\
\boldsymbol{\varepsilon}^{(2)} \cdot \mathbf{I}_1 &= -\sqrt{\frac{\pi}{2}} \sum_{l_\gamma=1} (-i)^{l_\gamma} \sqrt{2l_\gamma+1} \, \frac{i}{\sqrt{2}} \sum_{\mu=\pm1} \left[\mu \, p^M_{l_\gamma \mu} - i \, p^E_{l_\gamma \mu} \right],
\end{aligned} \tag{B17}$$

and summation over vectors of polarization is

$$\sum_{\alpha=1,2} \boldsymbol{\varepsilon}^{(\alpha)} \cdot \mathbf{I}_1 = -\sqrt{\frac{\pi}{2}} \sum_{l_\gamma=1} (-i)^{l_\gamma} \sqrt{2l_{\gamma+1}} \sum_{\mu=\pm1} \left[\frac{1+i\,\mu}{\sqrt{2}} \, p^M_{l_\gamma \mu} + \frac{1-i\,\mu}{\sqrt{2}} \, p^E_{l_\gamma \mu} \right]. \tag{B18}$$

There is the property

$$\begin{aligned}
\sum_{\mu=\pm1} \left[\frac{1-i\,\mu}{\sqrt{2}} \, p^E_{l_\gamma \mu} \right] &= \sum_{\mu=\pm1} \left[\frac{1+i\,\mu}{\sqrt{2}} \, p^E_{l_\gamma, -\mu} \right], \\
\sum_{\mu=\pm1} \left[\frac{1+i\,\mu}{\sqrt{2}} \, p^M_{l_\gamma \mu} + \frac{1-i\,\mu}{\sqrt{2}} \, p^E_{l_\gamma \mu} \right] &= \sum_{\mu=\pm1} \left[\frac{1+i\,\mu}{\sqrt{2}} \, p^M_{l_\gamma \mu} + \frac{1+i\,\mu}{\sqrt{2}} \, p^E_{l_\gamma, -\mu} \right] = \sum_{\mu=\pm1} \frac{1+i\,\mu}{\sqrt{2}} \left[p^M_{l_\gamma \mu} + p^E_{l_\gamma, -\mu} \right].
\end{aligned} \tag{B19}$$

Then one can write Eq. (B18) as

$$\sum_{\alpha=1,2} \boldsymbol{\varepsilon}^{(\alpha)} \cdot \mathbf{I}_1 = \sqrt{\frac{\pi}{2}} \sum_{l_\gamma=1} (-i)^{l_\gamma} \sqrt{2l_\gamma+1} \sum_{\mu=\pm1} \mu \, h_\mu \left(p^M_{l_\gamma, \mu} + p^E_{l_\gamma, -\mu} \right). \tag{B20}$$

We calculate properties

$$(\boldsymbol{\varepsilon}_x + \boldsymbol{\varepsilon}_z) \sum_{\alpha=1,2} [\mathbf{I}_1 \times \boldsymbol{\varepsilon}^{(\alpha)}] = \sqrt{\frac{\pi}{2}} \sum_{l_\gamma=1} (-i)^{l_\gamma} \sqrt{2l_\gamma+1} \sum_{\mu=\pm1} \mu \, h_\mu \left(p^M_{l_\gamma, \mu} - p^E_{l_\gamma, -\mu} \right). \tag{B21}$$

4. Case of $l_i = 0, l_f = 1, l_\gamma = 1$

In the case of $l_i = 0, l_f = 1, l_\gamma = 1$ integrals (B4) and (B7) are simplified to

$$\begin{aligned}
\mathbf{I}_1 &= -i\sqrt{\frac{3\pi}{2}} \sum_{\mu=\pm1} \boldsymbol{\xi}_\mu \, \mu \, \times \left[p^M_{l_\gamma \mu} - i\mu \, p^E_{l_\gamma \mu} \right], \quad I_3 = -i\sqrt{\frac{3\pi}{2}} \sum_{\mu=\pm1} \left[\mu \, \tilde{p}^M_{l_\gamma \mu}(c_A) - i \, \tilde{p}^E_{l_\gamma \mu}(c_A) \right], \\
I_2 &= -i\sqrt{\frac{3\pi}{2}} \sum_{\mu=\pm1} \left[\mu \, \tilde{p}^M_{l_\gamma \mu}(-c_p) - i \, \tilde{p}^E_{l_\gamma \mu}(-c_p) \right], \quad I_4 = -i\sqrt{\frac{3\pi}{2}} \sum_{\mu=\pm1} \left[\mu \, \breve{p}^M_{l_\gamma \mu}(c_A) - i \, \breve{p}^E_{l_\gamma \mu}(c_A) \right],
\end{aligned} \tag{B22}$$

where [see Eqs. (B4) and (B7)]

$$\begin{aligned}
p^M_{l_\gamma \mu} &= -I_M(0,1,1,1,\mu) J_1(0,1,1), \\
p^E_{l_\gamma \mu} &= \sqrt{\frac{2}{3}} I_E(0,1,1,1,0,\mu) J_1(0,1,0) - \sqrt{\frac{1}{3}} I_E(0,1,1,1,2,\mu) J_1(0,1,2), \\
\tilde{p}^M_{l_\gamma \mu}(c) &= \tilde{I}\,(0,1,1,1,\mu) \tilde{J}\,(c,0,1,1), \\
\tilde{p}^E_{l_\gamma \mu}(c) &= \sqrt{\frac{2}{3}} \tilde{I}\,(0,1,1,0,\mu) \tilde{J}\,(c,0,1,0) - \sqrt{\frac{1}{3}} \tilde{I}\,(0,1,1,2,\mu) \tilde{J}\,(c,0,1,2),
\end{aligned}$$

$$\breve{p}^{M}_{l_\gamma\mu}(c_A) = \tilde{I}\,(0,1,1,1,\mu)\breve{J}\,(c_A,0,1,1),$$
$$\breve{p}^{E}_{l_\gamma\mu}(c_A) = \sqrt{\frac{2}{3}}\tilde{I}\,(0,1,1,0,\mu)\breve{J}\,(c_A,0,1,0) - \sqrt{\frac{1}{3}}\tilde{I}\,(0,1,1,2,\mu)\breve{J}\,(c_A,0,1,2). \tag{B23}$$

The angular integrals are calculated in Appendix B in Ref. [44] [see Eqs. (B1)–(B10) in that paper]. The results of the calculation of angular integrals are

$$I_E\,(0,1,1,1,0,\mu) = \sqrt{\frac{1}{24\pi}}, \quad I_M\,(0,1,1,1,\mu) = 0, \quad I_E\,(0,1,1,1,2,\mu) = \frac{47}{240}\sqrt{\frac{3}{2\pi}},$$
$$\tilde{I}\,(0,1,1,0,\mu) = 0, \quad \tilde{I}\,(0,1,1,1,\mu) = \frac{\mu}{2\sqrt{2\pi}}, \quad \tilde{I}\,(0,1,1,2,\mu) = 0, \tag{B24}$$

and matrix elements (B23) are simplified to

$$p^{M}_{l_\gamma\mu} = 0, \quad p^{E}_{l_\gamma\mu} = \frac{1}{6}\sqrt{\frac{1}{\pi}}\cdot J_1(0,1,0) - \frac{47}{240}\sqrt{\frac{1}{2\pi}}\cdot J_1(0,1,2), \quad \tilde{p}^{M}_{1\mu}(c) = \frac{\mu}{2\sqrt{2\pi}}\cdot\tilde{J}\,(c,0,1,1), \quad \tilde{p}^{E}_{1\mu}(c) = 0,$$
$$\breve{p}^{M}_{1\mu}(c_A) = \frac{\mu}{2\sqrt{2\pi}}\cdot\breve{J}\,(c_A,0,1,1), \quad \breve{p}^{E}_{1\mu}(c_A) = 0. \tag{B25}$$

Now we calculate integrals in Eqs. (B25). For $p^{M}_{l_\gamma=1,\mu}$ and $p^{E}_{l_\gamma=1,\mu}$ we obtain

$$\mathbf{I}_1 = -i\sqrt{\frac{3\pi}{2}}\sum_{\mu=\pm1}\boldsymbol{\xi}_\mu\,\mu\,\times\left[-i\mu\,p^{E}_{l_\gamma=1,\,\mu}\right] = -\sqrt{\frac{3\pi}{2}}\,p^{E}_{l_\gamma=1,\,\mu}\,(\boldsymbol{\xi}_{-1}+\boldsymbol{\xi}_{+1}). \tag{B26}$$

Taking into account the summation of vectors of polarizations (B9),

$$\xi_{-1} = \frac{1}{\sqrt{2}}\,(\boldsymbol{\varepsilon}^{(1)} - i\boldsymbol{\varepsilon}^{(2)}), \quad \xi_{+1} = -\frac{1}{\sqrt{2}}\,(\boldsymbol{\varepsilon}^{(1)} + i\boldsymbol{\varepsilon}^{(2)}), \quad \xi_0 = \boldsymbol{\varepsilon}^{(3)},$$

we simplify Eq. (B26) as

$$\mathbf{I}_1 = -\sqrt{\frac{3\pi}{2}}\,p^{E}_{l_\gamma=1,\,\mu}(-i\sqrt{2}\,\boldsymbol{\varepsilon}^{(2)}) = i\sqrt{3\pi}\,p^{E}_{l_\gamma=1,\,\mu}\boldsymbol{\varepsilon}^{(2)}. \tag{B27}$$

From Eqs. (B17) we calculate products of integrals on vectors of polarizations:

$$\boldsymbol{\varepsilon}^{(1)}\cdot\mathbf{I}_1 = \left\{-\sqrt{\frac{\pi}{2}}\sum_{l_\gamma=1}(-i)^{l_\gamma}\sqrt{2l_\gamma+1}\,\frac{1}{\sqrt{2}}\sum_{\mu=\pm1}\left[p^{M}_{l_\gamma\mu} - i\,\mu\,p^{E}_{l_\gamma\mu}\right]\right\}_{l_\gamma=1}$$
$$= i\sqrt{\frac{\pi}{2}}\sqrt{\frac{3}{2}}\sum_{\mu=\pm1}\left[p^{M}_{l_\gamma=1,\mu} - i\,\mu\,p^{E}_{l_\gamma=1,\mu}\right] = i\,\frac{\sqrt{3\pi}}{2}\,p^{E}_{l_\gamma=1,\mu}\sum_{\mu=\pm1}(-i\,\mu\,) = 0, \tag{B28}$$

$$\boldsymbol{\varepsilon}^{(2)}\cdot\mathbf{I}_1 = \left\{-\sqrt{\frac{\pi}{2}}\sum_{l_\gamma=1}(-i)^{l_\gamma}\sqrt{2l_\gamma+1}\,\frac{i}{\sqrt{2}}\sum_{\mu=\pm1}\left[\mu\,p^{M}_{l_\gamma\mu} - i\,p^{E}_{l_\gamma\mu}\right]\right\}_{l_\gamma=1}$$
$$= -\sqrt{\frac{\pi}{2}}\sqrt{\frac{3}{2}}\sum_{\mu=\pm1}\left[\mu\,p^{M}_{l_\gamma=1,\mu} - i\,p^{E}_{l_\gamma=1,\mu}\right] = -\frac{\sqrt{3\pi}}{2}\sum_{\mu=\pm1}\left[-i\,p^{E}_{l_\gamma=1,\mu}\right] = i\sqrt{3\pi}\,p^{E}_{l_\gamma=1,\mu}. \tag{B29}$$

Therefore, we write down the final solutions:

$$\boldsymbol{\varepsilon}^{(1)}\cdot\mathbf{I}_1 = 0, \quad \boldsymbol{\varepsilon}^{(2)}\cdot\mathbf{I}_1 = \sum_{\alpha=1,2}\boldsymbol{\varepsilon}^{(\alpha)}\cdot\mathbf{I}_1 = i\sqrt{3\pi}\,p^{E}_{l_\gamma=1,\mu}. \tag{B30}$$

We obtain the property

$$\mathbf{I}_1 = i\sqrt{3\pi}\,p^{E}_{l_\gamma=1,\,\mu}\cdot\boldsymbol{\varepsilon}^{(2)} = \left[\sum_{\alpha=1,2}\boldsymbol{\varepsilon}^{(\alpha)}\cdot\mathbf{I}_1\right]\cdot\boldsymbol{\varepsilon}^{(2)}. \tag{B31}$$

Taking solution (B25) into account, rewritten via radial integrals,

$$p^{E}_{l_\gamma \mu} = \frac{1}{6}\sqrt{\frac{1}{\pi}} \cdot J_1(0,1,0) - \frac{47}{240}\sqrt{\frac{1}{2\pi}} \cdot J_1(0,1,2),$$

we obtain

$$\begin{aligned}
\mathbf{I}_1 &= \boldsymbol{\varepsilon}^{(2)} \cdot i\,\frac{\sqrt{3}}{6}\left\{J_1(0,1,0) - \frac{47}{40}\sqrt{\frac{1}{2}} \cdot J_1(0,1,2)\right\},\\
\boldsymbol{\varepsilon}^{(1)} \cdot \mathbf{I}_1 &= 0,\\
\boldsymbol{\varepsilon}^{(2)} \cdot \mathbf{I}_1 &= \sum_{\alpha=1,2} \boldsymbol{\varepsilon}^{(\alpha)} \cdot \mathbf{I}_1 = i\,\frac{\sqrt{3}}{6}\left\{J_1(0,1,0) - \frac{47}{40}\sqrt{\frac{1}{2}} \cdot J_1(0,1,2)\right\}.
\end{aligned} \tag{B32}$$

[1] M. Ya. Amusia, "Atomic" bremsstrahlung, Phys. Rep. **162**, 249 (1988).

[2] V. A. Pluyko and V. A. Poyarkov, Bremsstrahlung in reactions induced by protons, Phys. El. Part. At. Nucl. **18**, 374 (1987).

[3] V. V. Kamanin, A. Kugler, Y. E. Penionzhkevich, I. S. Batkin, and I. V. Kopytin, High-energy gamma-ray emission in heavyion reactions at nonrelativistic energies, Phys. Elem. Part. At. Nucl. **20**, 743 (1989).

[4] C. A. Bertulani and G. Baur, Electromagnetic processes in relatevistic heavy ion collisions, Phys. Rep. **163**, 299 (1988).

[5] S. P. Maydanyuk and V. S. Olkhovsky, Angular analysis of bremsstrahlung in α-decay, Eur. Phys. J. A **28**, 283 (2006).

[6] S. P. Maydanyuk and V. S. Olkhovsky, Does sub-barrier bremsstrahlung in α-decay of ^{210}Po exist? Prog. Theor. Phys. **109**, 203 (2003).

[7] S. P. Maydanyuk, V. S. Olkhovsky, G. Giardina, G. Fazio, G. Mandaglio, and M. Manganaro, Bremsstrahlung emission accompanying α-decay of deformed nuclei, Nucl. Phys. A **823**, 38 (2009).

[8] S. P. Maydanyuk, Multipolar model of bremsstrahlung accompanying proton decay of nuclei, J. Phys. G **38**, 085106 (2011).

[9] S. P. Maydanyuk, V. S. Olkhovsky, G. Mandaglio, M. Manganaro, G. Fazio, and G. Giardina, Bremsstrahlung emission of high energy accompanying spontaneous of ^{252}Cf, Phys. Rev. C **82**, 014602 (2010).

[10] S. P. Maydanyuk, V. S. Olkhovsky, G. Mandaglio, M. Manganaro, G. Fazio, and G. Giardina, Bremsstrahlung emission of photons accompanying ternary fission of ^{252}Cf, J. Phys.: Conf. Ser. **282**, 012016 (2011).

[11] S. P. Maydanyuk, P.-M. Zhang, and L.-P. Zou, Manifestation of the important role of nuclear forces in the emission of photons in pion scattering off nuclei, Phys. Rev. C **98**, 054613 (2018).

[12] S. Pastore, R. Schiavilla, and J. L. Goity, Electromagnetic two-body currents of one- and two-pion range, Phys. Rev. C **78**, 064002 (2008).

[13] D. Baye and P. Descouvemont, Microscopic description of nucleus-nucleus bremsstrahlung, Nucl. Phys. A **443**, 302 (1985).

[14] Q. K. K. Liu, Y. C. Tang, and H. Kanada, Microscopic calculation of bremsstrahlung emission in ^{3}He $+\alpha$ collisions, Phys. Rev. C **41**, 1401 (1990).

[15] Q. K. K. Liu, Y. C. Tang, and H. Kanada, Microscopic study of $p+\alpha$ bremsstrahlung, Phys. Rev. C **42**, 1895 (1990).

[16] D. Baye, C. Sauwens, P. Descouvemont, and S. Keller, Accurate treatment of Coulomb contribution in nucleus-nucleus bremsstrahlung, Nucl. Phys. A **529**, 467 (1991).

[17] Q. K. K. Liu, Y. C. Tang, and H. Kanada, Approximate treatment of antisymmetrization in the microscopic studies of $p+\alpha$ and ^{3}He $+\alpha$ bremsstrahlung, Phys. Rev. C **44**, 1695 (1991).

[18] D. Baye, P. Descouvemont, and M. Kruglanski, Probing scattering wave functions with nucleus-nucleus bremsstrahlung, Nucl. Phys. A **550**, 250 (1992).

[19] Q. K. K. Liu, Y. C. Tang, and H. Kanada, Microscopic study of $\alpha+\alpha$ bremsstrahlung with resonating-group wave functions, Few-Body Syst. **12**, 175 (1992).

[20] M. Kruglanski, D. Baye, and P. Descouvemont, Alpha-alpha bremsstrahlung in a microscopic model, in *Nuclei in the Cosmos 2*, edited by F. Kaeppeler and K. Wisshak (IOP, Bristol, 1993), pp. 423–428.

[21] J. Dohet-Eraly, J.-M. Sparenberg, and D. Baye, Microscopic calculations of elastic scattering between light nuclei based on a realistic nuclear interaction J. Phys.: Conf. Ser. **321**, 012045 (2011).

[22] J. Dohet-Eraly and D. Baye, Microscopic cluster model of $\alpha+n$, $\alpha+p$, $\alpha+$He^3, and $\alpha+\alpha$ elastic scattering from a realistic effective nuclear interaction, Phys. Rev. C **84**, 014604 (2011).

[23] J. Dohet-Eraly and D. Baye, Siegert approach within a microscopic description of nucleus-nucleus bremsstrahlung Phys. Rev. C **88**, 024602 (2013).

[24] J. Dohet-Eraly, D. Baye, and P. Descouvemont, Microscopic description of $\alpha+\alpha$ bremsstrahlung from a realistic nucleon-nucleon interaction J. Phys.: Conf. Ser. **436**, 012030 (2013).

[25] J. Dohet-Eraly, Microscopic cluster model of elastic scattering and bremsstrahlung of light nuclei, Ph.D. thesis, Universite Libre De Bruxelles, 2013.

[26] J. Dohet-Eraly, Microscopic description of $\alpha+N$ bremsstrahlung by a Siegert approach, Phys. Rev. C **89**, 024617 (2014).

[27] J. Dohet-Eraly and D. Baye, Comparison of potential models of nucleus-nucleus bremsstrahlung, Phys. Rev. C **90**, 034611 (2014).

[28] S. P. Maydanyuk and V. S. Vasilevsky, Systematic study of bremsstrahlung emission in reactions with light nuclei in cluster models, Phys. Rev. C **108**, 064001 (2023).

[29] G. F. Filippov and I. P. Okhrimenko, Use of an oscillator basis for solving continuum problems, Sov. J. Nucl. Phys. **32**, 480 (1981).

[30] G. F. Filippov, Taking into account correct asymptotic behavior in oscillator-basis expansions, Sov. J. Nucl. Phys. **33**, 488 (1981).
[31] V. S. Vasilevsky, F. Arickx, J. Broeckhove, and T. P. Kovalenko, A microscopic three-cluster model with nuclear polarization applied to the resonances of ^{7}Be and the reaction ^{6}Li(p, ^{3}He) ^{4}He, Nucl. Phys. A **824**, 37 (2009).
[32] J. M. Eisenberg and W. Greiner, *Excitation Mechanisms of the Nucleus* (North-Holland, Amsterdam, 1970).
[33] D. R. Thompson, M. LeMere, and Y. C. Tang, Systematic investigation of scattering problems with the resonating-group method, Nucl. Phys. A **286**, 53 (1977).
[34] Y. N. Demkov and V. N. Ostrovskii, *Zero-Range Potentials and Their Applications in Atomic Physics* (Springer, New York, 1988).
[35] Y. A. Lashko, G. F. Filippov, and V. S. Vasilevsky, Dynamics of two-cluster systems in phase space, Nucl. Phys. A **941**, 121 (2015).
[36] N. Kalzhigitov, V. O. Kurmangaliyeva, N. Z. Takibayev, and V. S. Vasilevsky, Resonance structure of ^{8}Be within the two-cluster resonating group method, Ukr. J. Phys. **68**, 3 (2023).
[37] A. B. Volkov, Equilibrum deformation calculation of the ground state energies of 1p shell nuclei, Nucl. Phys. **74**, 33 (1965).
[38] A. Hasegawa and S. Nagata, Ground state of ^{6}Li, Prog. Theor. Phys. **45**, 1786 (1971).
[39] F. Tanabe, A. Tohsaki, and R. Tamagaki, $\alpha\alpha$ scattering at intermediate energies: Applicability of orthogonality condition model and upper limit of isoscalar meson-nucleon coupling constants inferred from potential tail, Prog. Theor. Phys. **53**, 677 (1975).
[40] J. Clayton, W. Benenson, M. Cronqvist, R. Fox, D. Krofcheck, R. Pfaff, T. Reposeur, J. D. Stevenson, J. S. Winfield, B. Young, M. F. Mohar, C. Bloch, and D. E. Fields, Proton-deuteron bremsstrahlung at 145 and 195 MeV, Phys. Rev. C **45**, 1810 (1992).
[41] V. Herrmann, J. Speth, and K. Nakayama, Nucleon-nucleon bremsstrahlung at intermediate energies, Phys. Rev. C **43**, 394 (1991).
[42] C. Ernst, S. A. Bass, M. Belkacem, H. Stöcker, and W. Greiner, Intermediate mass excess of dilepton production in heavy ion collisions at relativistic energies, Phys. Rev. C **58**, 447 (1998).
[43] W. K. Wilson *et al.*, Inclusive dielectron cross sections in p+p and p+d interactions at beam energies from 1.04 to 4.88 GeV, Phys. Rev. C **57**, 1865 (1998).
[44] S. P. Maydanyuk, Model for bremsstrahlung emission accompanying interactions between protons and nuclei from low energies up to intermediate energies: Role of magnetic emission, Phys. Rev. C **86**, 014618 (2012).
[45] K. Nakayama, Hard photon production in proton-deuteron reactions at intermediate energies, Phys. Rev. C **45**, 2039 (1992).
[46] S. P. Maydanyuk, P.-M. Zhang, and L.-P. Zou, Nucleon microscopy in proton-nucleus scattering via analysis of bremsstrahlung emission, Phys. Rev. C **99**, 064602 (2019).